

Artificial Neural Networks based Modeling & Analysis of
Semi-Active Damper System

Nishant Bhanot

Thesis submitted to the faculty of the Virginia Polytechnic Institute and State
University in partial fulfillment of the requirements for the degree of

Master of Science

In

Mechanical Engineering

Saied Taheri (Chair)

John B. Ferris

Corina Sandu

May 8th, 2017

Blacksburg, VA

Keywords: artificial neural network, semi active, damper, suspension, quarter car
simulation, control, Simulink, CarSim

Copyright 2017, Nishant Bhanot

Artificial Neural Networks based Modeling & Analysis of Semi-Active Damper System

Nishant Bhanot

ABSTRACT

The suspension system is one of the most sensitive systems of a vehicle as it affects the dynamic behavior of the vehicle with even minor changes. These systems are designed to carry out multiple tasks such as isolating the vehicle body from the road/tire vibrations as well as achieving desired ride and handling performance levels in both steady state and limit handling conditions. The damping coefficient of the damper plays a crucial role in determining the overall frequency response of the suspension system. Considerable research has been carried out on semi active damper systems as the damping coefficient can be varied without the system requiring significant external power giving them advantages over both passive and fully active suspension systems.

Dampers behave as non-linear systems at higher frequencies and hence it has been difficult to develop accurate models for its full range of motion. This study aims to develop a velocity sensitive damper model using artificial neural networks and essentially provide a 'black-box' model which encapsulates the non-linear behavior of the damper. A feed-forward neural network was developed by testing a semi active damper on a shock dynamometer at CenTiRe for multiple frequencies & damping ratios. This data was used for supervised training of the network using MATLAB Neural Network Toolbox. The developed NN model was evaluated for its prediction accuracy. Further, the developed damper model was analyzed for feasibility of use for simulations & controls by integrating it in a Simulink based quarter car model and applying the well-known skyhook control strategy. Finally, effects on ride and handling dynamics were evaluated in Carsim by replacing the default damper model with the proposed model. It was established that this damper modeling technique can be used to help evaluate the behavior of the damper on both component as well as vehicle level without needing to develop a complex physics based model. This can be especially beneficial in the earlier stages of vehicle development.

Artificial Neural Networks based Modeling & Analysis of Semi-Active Damper System

Nishant Bhanot

GENERAL AUDIENCE ABSTRACT

The suspension system is one of the most sensitive systems of a vehicle as it affects the dynamic behavior of the vehicle with even minor changes. These systems are designed to carry out multiple tasks such as absorbing shocks from the road as well as improving the handling of the vehicle for a smoother and safer drive. The level of firmness of the shock absorber/damper plays a crucial role in determining the overall behavior of the suspension system. Considerable research has been carried out on semi active damper systems as the damper stiffness can be varied quickly and easily as compared to other passive and fully active damper systems.

Dampers are complex systems to model especially for high speed operations and hence it has been difficult to develop accurate mathematical models for its full range of motion. This study aims to develop an accurate mathematical model for a semi active damper using artificial neural networks. A semi active damper was fabricated and tested on a shock dynamometer at CenTiRe for multiple speeds and stiffness values. This test data obtained was used for training of the mathematical model using the computer software MATLAB. The developed model was evaluated for its accuracy and further analyzed for feasibility of use in computer simulations. It was established that this damper modeling technique can be used to help evaluate the behavior of the damper with high accuracy while still running the simulations relatively quickly whereas in current simulations compromise has to be made on at least the accuracy of the model or the simulation speed. This can be especially beneficial in the earlier stages of vehicle development.

ACKNOWLEDGEMENTS

First and foremost, I would like to thank my graduate advisor, Dr. Saied Taheri, who has always shown faith in me and consistently guided me all throughout graduate school. His patience, attitude and demeanor are inspiring. He has always been extremely supportive and open to ideas throughout my research while constantly driving me in the right direction when necessary. I could not have asked for a better advisor than him.

I would also like to thank Dr. Ferris and Dr. Sandu for serving as my graduate thesis committee members and making significant suggestions to improve my research.

I thoroughly enjoyed the company of my labmates and my time being a part of CenTiRe at Virginia Tech. I'd like to thank Omid Ghasemalizadeh for shaping my research while working with me on using concepts of neural networks & suspensions and Sheetanshu Tyagi for helping to set up the complete test rig. I also want to thank Anup Cherukuri for the detailed discussions on vehicle dynamics concepts. A big thanks to all those who were directly or indirectly involved in the research work.

Lastly, I would like to thank my parents who always believed in me and without whom I would not have been here today. I could only succeed in graduate school due to their love and emotional support. I would like to mention my uncle's family in Virginia and thank them for giving me a home away from home. My family is the source of my strength and determination.

CONTENTS

ABSTRACT.....	ii
GENERAL AUDIENCE ABSTRACT.....	iii
ACKNOWLEDGEMENTS.....	iv
LIST OF FIGURES	vii
LIST OF TABLES.....	ix
NOMENCLATURE	x
1 INTRODUCTION	1
1.1 Background.....	2
1.1.1 Passive Suspension	3
1.1.2 Semi - Active Suspension	4
1.1.3 Active Suspension.....	5
1.2 Semi Active Dampers	7
1.2.1 Electrohydraulic Valve Control	7
1.2.2 Magnetorheological Fluid Control.....	8
1.2.3 Electrorheological Fluid Control.....	9
1.3 Damper Modeling.....	10
1.4 Motivation.....	12
1.5 Objective of Thesis	12
1.6 Thesis Outline	13
2 ARTIFICIAL NEURAL NETWORKS	15
2.1 Introduction.....	15
2.2 Training of a neural network.....	16
2.3 Learning Algorithms	19
2.3.1 Levenberg – Marquardt.....	19
2.3.2 Bayesian Regularization	20

2.3.3	Scaled Conjugate.....	21
2.4	Advantages & Limitations	21
2.5	MATLAB neural network toolbox	22
3	DAMPER FABRICATION, SETUP AND TESTING.....	26
3.1	Semi Active Damper Setup and Control.....	26
3.2	Testing Setup	27
3.3	Damper Testing and Data Collection.....	30
4	ARCHITECTURE, TRAINING AND EVALUATION OF ANN MODEL	39
4.1	Introduction.....	39
4.2	Data Processing for ANN Training.....	40
4.3	ANN Training and Validation.....	41
4.4	Summary and Discussion.....	44
5	SIMULATIONS AND RESULTS.....	46
5.1	Quarter Car Simulations.....	46
5.1.1	Quarter Car Model Development.....	46
5.1.2	Tests and Results.....	50
5.2	Full Vehicle Simulations.....	59
5.2.1	CarSim Model Development	59
5.2.2	Tests and Results.....	61
6	CONCLUSIONS AND FUTURE WORK	66
	BIBLIOGRAPHY	69

LIST OF FIGURES

Figure 1: Ride Comfort vs Vehicle Handling compromise for passive damper systems	2
Figure 2: Commercial Passive Suspension System	2
Figure 3: Quarter Car Models for Suspension Systems (a) Passive (b) Semi-Active (c) Active.....	3
Figure 4: Transfer Function frequency response (a) road to vehicle body (b) road to tire	4
Figure 5: Commercial Semi-Active Suspension system.....	5
Figure 6: Bose Electromagnetic Active Suspension System Prototype.....	6
Figure 7: Classification of controllable suspension systems.....	6
Figure 8: Semi-Active Dampers (a) Electrohydraulic (b) Magnetorheological (c) Electrorheological	7
Figure 9: Electrohydraulic Semi Active Damper Schematic (a) variable internal orifice (b) external by-pass valve	8
Figure 10: MR Damper schematic (magnetic field represented by B)	9
Figure 11: ER Damper schematic (magnetic field represented by E).....	10
Figure 12: Schematic representation for MR damper modeling	11
Figure 13: Typical feedforward network (left) and a recurrent network (right)	16
Figure 14: Single Neuron Input and Output Architecture.....	17
Figure 15: Net Input to Neuron with bias	18
Figure 16: Neural Network Start Dialog Box	22
Figure 17: Input and Target data selection from MATLAB workspace	22
Figure 18: Division of Dataset for Training, Validation and Testing	23
Figure 19: Selection of neurons for network architecture.....	24
Figure 20: Deploy Neural Network	24
Figure 21: Semi Active Damper	26
Figure 22: HydraForce SP10-24 solenoid valve	27
Figure 23: HydraForce Controller-0101A	27
Figure 24: Testing and Data Collection Diagram	28
Figure 25: Testing and Data collection setup at CenTiRe	28
Figure 26: Controller calibration (top) and valve specifications (bottom).....	29
Figure 27: LabVIEW Program for valve control	30
Figure 28: Repeatability Test Results (0.25 Hz-3 Hz).....	31
Figure 29: Temperature Variation Test Results (0.25 Hz - 1 Hz).....	32
Figure 30: Damper Characteristics at 0.25 Hz - F vs X (Top) & F vs V (Bottom).....	35
Figure 31: Damper Characteristics at 1 Hz - F vs X (Top) & F vs V (Bottom).....	36

Figure 32: Damper Characteristics at 2 Hz - F vs X (Top) & F vs V (Bottom).....	37
Figure 33: Damper Characteristics at 3 Hz - F vs X (Top) & F vs V (Bottom).....	38
Figure 34: Developed ANN Architecture	40
Figure 35: Error Distribution for Damper Force.....	42
Figure 36: Predicted vs Actual Force at 0.25 Hz	43
Figure 37: Predicted vs Actual Force at 1 Hz	43
Figure 38: Predicted vs Actual Force at 2 Hz	43
Figure 39: Predicted vs Actual Force at 3 Hz	44
Figure 40: Point Contact Quarter Car Model.....	47
Figure 41: Simulink Quarter Car Model Architecture	48
Figure 42: ANN Damper Model Integration.....	48
Figure 43: Lookup Table Damper Model	50
Figure 44: Simulation Inputs (a) Impulse (b) Sine Sweep (c) Road Profile	51
Figure 45: Sprung Mass Impulse Response – Low Damping Mode.....	52
Figure 46: Sprung Mass Impulse Response – High Damping Mode.....	52
Figure 47: Sprung Mass Sine Sweep Response – Low Damping Mode.....	53
Figure 48: Sprung Mass Sine Sweep Response – High Damping Mode	53
Figure 49: Sprung Mass Road Response at 10m/s – Low Damping Mode	55
Figure 50: Sprung Mass Road Response at 10m/s – High Damping Mode.....	55
Figure 51: Sprung Mass Road Response at 20m/s – Low Damping Mode	56
Figure 52: Sprung Mass Road Response at 20m/s – High Damping Mode.....	56
Figure 53: Sprung Mass Road Response at 10m/s – Skyhook Control	57
Figure 54: Sprung Mass Road Response at 20m/s – Skyhook Control	57
Figure 55: SIL Setup using CarSim with MATLAB/Simulink	59
Figure 56: Actual CarSim-Simulink Setup	60
Figure 57: (a) CarSim Setup (b) Low Damping Lookup Table Damper	61
Figure 58: Tests carried out in CarSim: (a) BSST (b) DLC (c) DLC (Top View)	62
Figure 59: Vehicle Body Acceleration -BSST (a) Low Damping Mode (b) High Damping Mode	63
Figure 60: DLC Test Results – Low Damping:(a),(c),(e),(g) High Damping:(b),(d),(f),(h)	65

LIST OF TABLES

Table 1: Typical Analytic Activation Functions 18

Table 2: Semi Active Damper Testing Plan for 2-inch stroke 33

Table 3: Comparison of Learning Algorithms 41

Table 4: ANN Prediction error table 44

Table 5: Quarter Car Parameter Definition 47

Table 6: Sprung mass acceleration and displacement dynamics for sine sweep test 54

Table 7: Acceleration RMS values for rough road input 58

NOMENCLATURE

ANN	Artificial Neural Network
BR	Bayesian Regularization
BSST	Bounce Sine Sweep Test
DLC	Double Lane Change
EH	Electrohydraulic
EHM	Elementary Hysteresis Model
ER	Electrorheological
FCC	Fully Connected Cascade
FNN	Feedforward Neural Network
GN	Gauss-Newton
HIL	Hardware-in-the-Loop
LM	Levenberg-Marquardt
MLP	Multi-Layer Perceptron
MR	Magnetorheological
MSE	Mean Squared Error
NN	Neural Network
RBF	Radial Basis Function
RMS	Root Mean Square
RNN	Recurrent Neural Network
RWD	Rear Wheel Drive
SC	Scaled Conjugate
SIL	Software-in-the-Loop

1 INTRODUCTION

An automotive suspension system is one of the most important components of a vehicle. The major aims of a typical vehicle suspension are: (a) vehicle body isolation from the external disturbance due to the road surface and internal disturbances due to yaw, pitch and roll of the body; (b) support vehicle body weight; (c) react to vehicle weight variations due to change in passenger or luggage weight to maintain desired vehicle dynamics; (d) ensure road-tire contact to maintain vehicle road holding capabilities [1]. Therefore, suspension systems play a key role in defining the ride and handling dynamics of a vehicle. When designing a conventional passive suspension system, there has always been an inherent trade-off between the ride comfort and vehicle stability performance indexes as shown in Figure 1 [2]. For such conventional systems, with high vehicle stability comes a relatively uncomfortable ride and conversely with soft & smooth ride comes poor vehicle handling and stability during maneuvering. Previous literature also highlights the importance of suspension system design for vehicle safety and ride comfort [3, 4]. To overcome these challenges multiple semi active and active suspension systems have been developed along with effective control strategies which can make the vehicle suspension system alter its behavior in real time to provide the needed response at multiple instances of time. To design vehicle suspension systems, knowledge of the behavior of the damper is of prime importance. The damper, which is sometimes also referred to as the shock absorber, is responsible for dissipating unwanted energy in the form of heat [5]. This energy is introduced into the system due to either road disturbances or vehicle body motion. Accurate damper modeling has been of prime focus since the development of modern suspension systems. For basic analysis, damper force is considered to be proportional to the relative velocity of the piston. However, dampers are inherently non-linear systems especially at higher frequencies. Multiple modeling techniques have been proposed over the years to help develop accurate damper models which can be used for damper tuning. Vehicle simulations carried out using these damper models are moderately dependable but as of recent times, damper tuning for desired vehicle performance is still largely based on trial and error on the track and is hence casually referred to as ‘black art tuning’. Therefore, there is a need in the industry to explore techniques which can help develop accurate and computationally inexpensive damper models with relative ease which can be further used in full vehicle simulations.

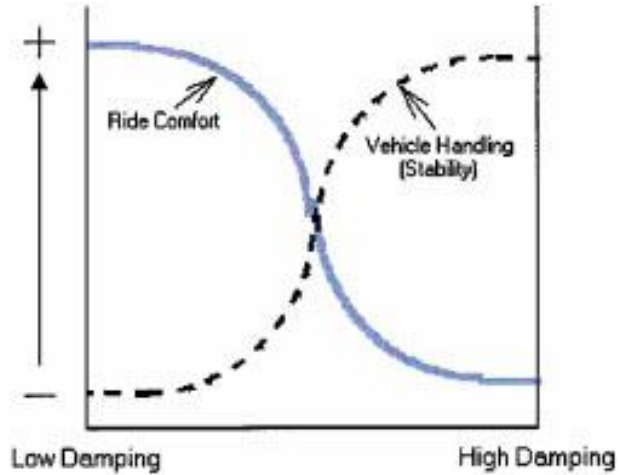


Figure 1: Ride Comfort vs Vehicle Handling compromise for passive damper systems

Used under Fair Use 2017 [2]

1.1 Background

A typical vehicle suspension system primarily consists of springs, dampers, mechanical linkages and elasto-kinematic joints. This complex setup has a significant impact on the vehicle motion. Figure 2 shows a commercial passive suspension system.

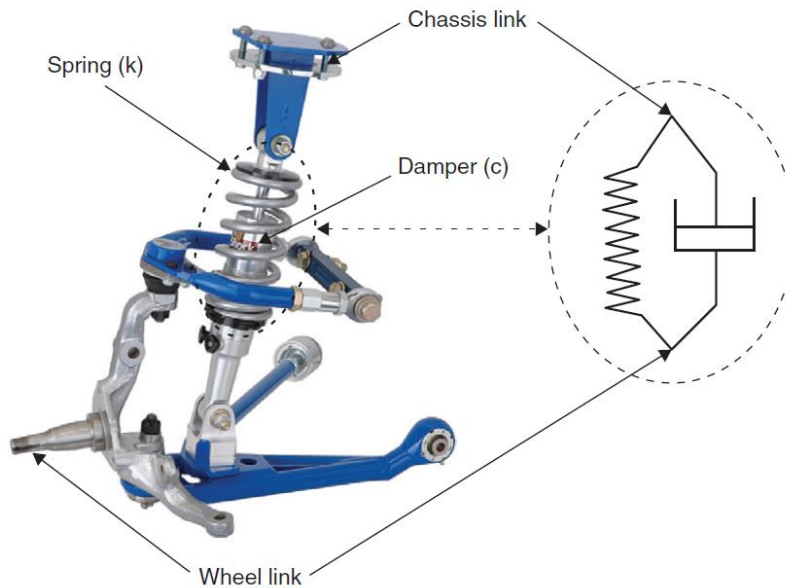


Figure 2: Commercial Passive Suspension System

Used under Fair Use 2017 [6]

As stated before, the dampers of the suspension system play a crucial role in controlling this vehicle motion. Based on the damping control and actuation capabilities, vehicle suspension systems can be categorized into three categories: (a) passive (b) semi-active (c) active. Figure 3 shows the quarter car models generally used to represent these systems. The key differences due to the variable damper and force actuators can be observed through these models and as described in the following sections.

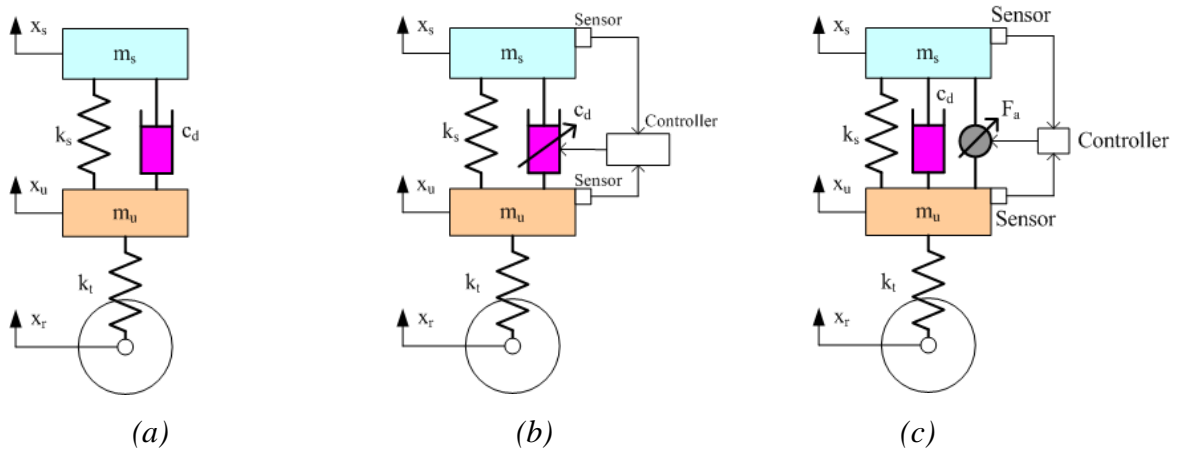


Figure 3: Quarter Car Models for Suspension Systems (a) Passive (b) Semi-Active (c) Active

Used under Fair Use 2017 [1]

1.1.1 Passive Suspension

A passive suspension is a conventional system consisting of a spring (linear or progressive) and a damper for shock absorption and energy dissipation. Both components work in parallel and are fixed between the vehicle body and the wheel supporting structure. During relative displacement between the body and the wheel, the damper exerts an opposing force approximately proportional to the relative velocity of compression or rebound. In Figure 3(a) the quarter car model represents a passive suspension system where m_s is the sprung mass i.e vehicle body, m_u is the unsprung mass i.e wheel support structure, k_s represents the suspension spring stiffness, k_t represents the tire stiffness, C_d represents the damping coefficient, x_r represents the road disturbance vertical displacement, x_u represents unsprung mass vertical displacement and x_s represents the sprung mass vertical displacement. Passive damper systems are a popular choice for vehicles due to their

simplicity, small volumes, low costs and low maintenance. They do not allow any outside control and hence improvements are possible only in the field of shapes, hole valves and materials [7]. Figure 4 shows a typical frequency response of the transfer function between (a) road to vehicle body and (b) road to tire. Changing the damping coefficient with change in disturbance frequency can have a major effect on the vehicle body displacement and hence passive dampers are not the best solution to maximize ride comfort.

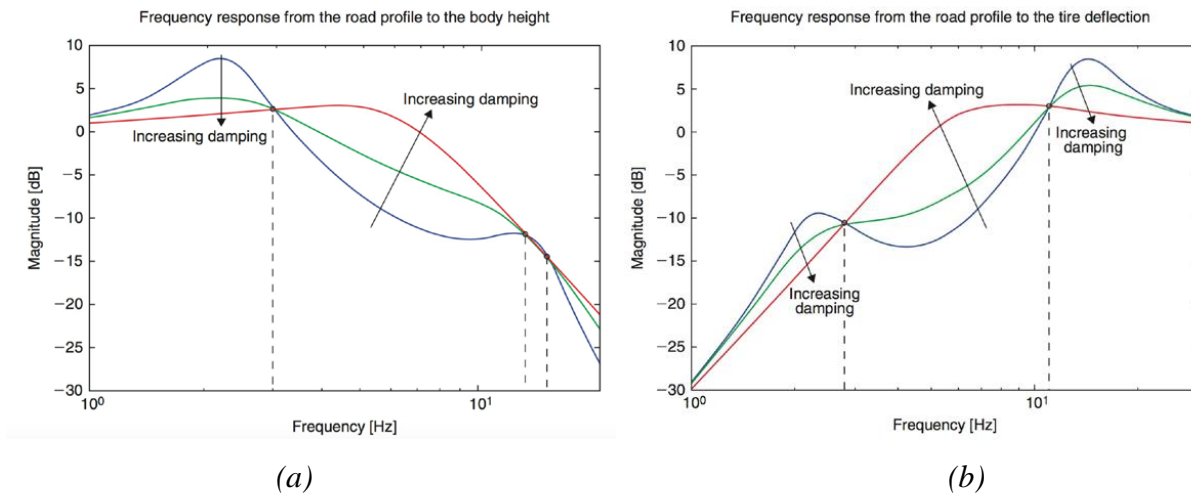


Figure 4: Transfer Function frequency response (a) road to vehicle body (b) road to tire

Used under Fair Use 2017[6]

1.1.2 Semi - Active Suspension

A semi- active suspension system is one in which the damper has the capability to vary its damping coefficient. In general, the mechanical setup of a semi-active suspension system is similar to that of a passive suspension system except for an electrically/magnetically controlled damper capable of providing varying damping. Figure 3(b) shows a quarter car model of a semi active suspension system and as it can be observed, the only difference is the damper with variable damping capability fitted in a close loop control using sensors. Essentially, a semi-active damper can be set up to change from soft to stiff damping or vice versa using a controller, which can affect the vehicle body displacement and accelerations based on the transfer function response as illustrated in Figure 4. This study used a semi- active damper for all the analysis, testing & data collection, model development and simulations. Semi- active dampers and their types have been discussed in more

details in Section 1.2. Figure 5 shows the basic setup of a semi-active suspension system.

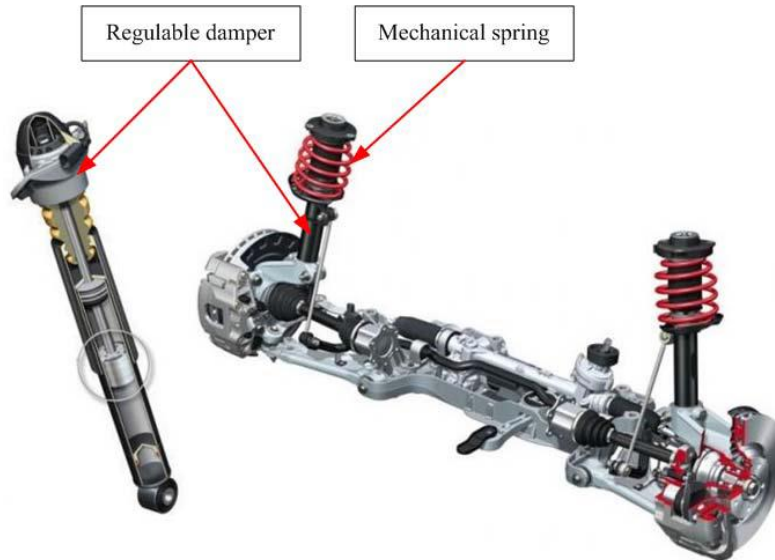


Figure 5: Commercial Semi-Active Suspension system

Used under Fair Use 2017 [1]

1.1.3 Active Suspension

The major shortcoming of a semi - active damper is that it does not have the capability to actively apply force to the vehicle body or the wheel supporting structure. To overcome this shortcoming, active suspension systems have been developed. Just like passive suspension systems, an active suspension system consists of a spring and damper but also contains a force actuator; usually hydraulic, pneumatic or electromagnetic in nature. Figure 3(c) illustrates a quarter car model for an active suspension system. An additional force actuator F_a can be observed to be fitted the sprung and unsprung masses. This force actuator can apply force on the vehicle body and wheel support structure as per the controller demand. The controller is driven by a control algorithm and the sensors attached to the vehicle to obtain the desired characteristics. Although the cost of implementation of an active suspension is the highest when compared to passive or semi-active suspensions, the system has immense potential for future research. Ekchian, J., et al [8] proposed a high bandwidth active suspension system to reduce motion sickness experienced by the passenger which is expected to rise significantly as autonomous vehicles move closer to reality.

Due to active force introduction capabilities, the applications of active suspension systems are immense, provided cost and power availability are not a limitation. Figure 6 shows a prototype active suspension system.



Figure 6: Bose Electromagnetic Active Suspension System Prototype

Used under Fair Use 2017 [1]

Now that all types of suspension systems have been discussed, a classification of the controllable suspension systems has been illustrated in Figure 7.

System class	Control range (spring)	Control range (damper)	Control bandwidth	Power request	Control variable
Passive			-	-	-
Adaptive			1-5 Hz	10-20 W	c (damping ratio)
Semi-active			30-40 Hz	10-20 W	c (damping ratio)
Load leveling			0.1-1 Hz	100-200 W	W (static load)
Slow active			1-5 Hz	1-5 kW	F (force)
Fully active			20-30 Hz	5-10 kW	F (force)

Figure 7: Classification of controllable suspension systems

Used under Fair Use 2017[6]

1.2 Semi Active Dampers

As discussed in the previous sections, a semi active suspension system consists of a damper capable of varying its damping coefficient as governed by a control algorithm. The objective of the algorithm is to change the damper characteristics as per the immediate need of either maintaining superior ride comfort, vehicle handling or a combination of both. Multiple methods have been developed to vary the damping coefficient electronically by either changing the damper fluid characteristics or changing the resistance of fluid flow within the damper. These designs have been briefly discussed below and illustrated in Figure 8. For this study an electrohydraulic valve control type semi-active damper was used.

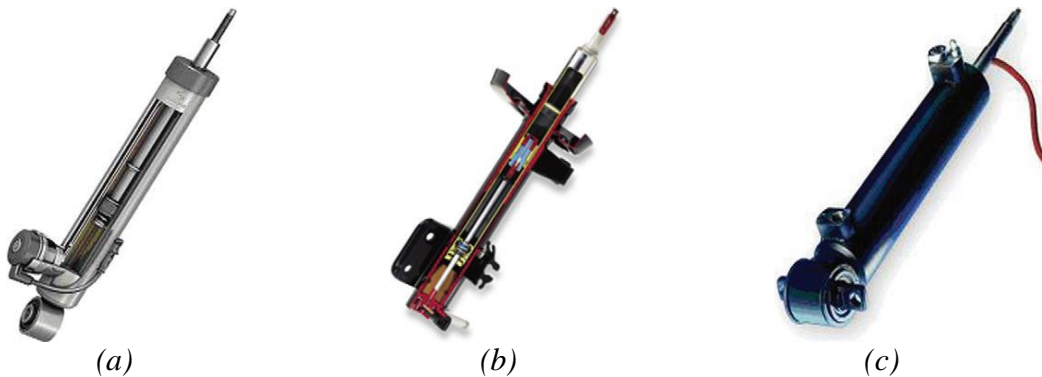


Figure 8: Semi-Active Dampers (a) Electrohydraulic (b) Magnetorheological (c) Electrorheological

Used under Fair Use 2017[6]

1.2.1 Electrohydraulic Valve Control

Electrohydraulic (EH) valve type dampers work on the principle of varying the resistance the fluid inside the damper experiences while moving from one chamber to the other. This resistance can be varied by either varying the orifice diameters in the piston or by providing alternate paths for fluid flow through a by-pass valve controlled by a solenoid valve. The orifice or solenoid valve opening is controlled by providing power command through a controller. This technique can provide high speed, accurate flow control at high operating pressures [9]. One of the major advantages of this design is low cost and power demand for implementation and operation. The construction of the semi-active damper, solenoid valve and controller has been discussed in

Chapter 3. Figure 9 shows typical schematics for EH semi-active dampers.

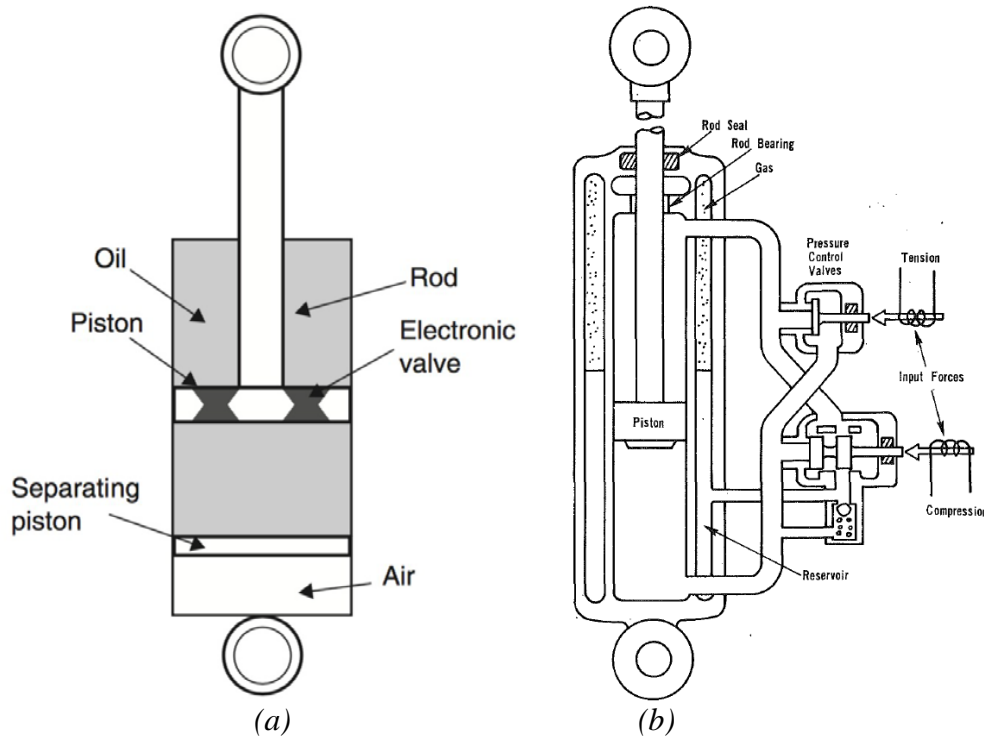


Figure 9: Electrohydraulic Semi Active Damper Schematic (a) variable internal orifice (b) external by-pass valve

Used under Fair Use 2017 [6, 9]

1.2.2 Magnetorheological Fluid Control

Magnetorheological damper systems consist of a non-Newtonian MR fluid that can change its viscosity when magnetic field is varied across the damper. The MR fluid contains micron-size iron particles suspended in a petroleum or silica based carrier fluid oil. When magnetic field is applied across this fluid, the iron particles align in chain-like structures along the flux lines and thus changing the rheological properties of the fluid. This causes the fluid to exhibit varying viscosity and the damper varies the resistive force it applies to the sprung and unsprung vehicle mass. Various studies have been carried out to develop damper models and validate them using experimental testing. Farjoud, A [10] presented a physics based MR damper model and discussed possible applications for reliable advanced suspension systems. Commercialization of MR dampers has been slow due to requirement of large volume MR fluid making it expensive and

heavy for industrial implementation. Particle settling, field saturation and wall effects have limited the scope of the current commercial implementation of these systems. Although, MR dampers have low response times, the increase of cost and power requirements for implementation was the major motivation for choosing an electrohydraulic damper over an MR damper for this study. Figure 10 shows a schematic for a typical MR damper construction and working principle.

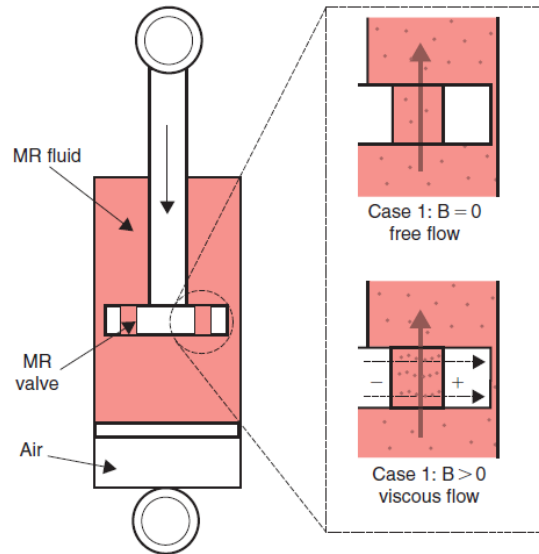


Figure 10: MR Damper schematic (magnetic field represented by B)

Used under Fair Use 2017[6]

1.2.3 Electrorheological Fluid Control

Electrorheological (ER) damper systems are like MR dampers except that the ER fluid inside the damper changes viscosity with the application of an electric field instead of a magnetic field. ER dampers are essentially ‘electric capacitors’ with the external body acting as the anode and the piston being the cathode. To obtain the required magnitude of damper force, relatively large pistons are preferred. Like the MR dampers, they require higher power for operation; typically, 1-5kV. They are also heavy and sensitive to temperature changes and are hence not commercially used extensively. Figure 8(c) shows an ER damper. Figure 11 shows a schematic for a typical ER damper construction and working principle.

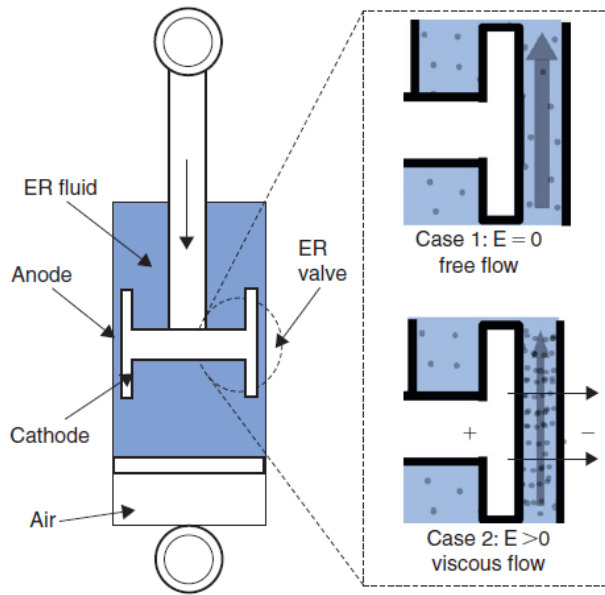


Figure 11: ER Damper schematic (magnetic field represented by E)

Used under Fair Use 2017[6]

1.3 Damper Modeling

Damper modeling has been the focus of many studies due to the sheer complexity of the dynamics involved. For basic analysis, modern dampers are considered to exhibit a force response proportional to the relative velocity of compression or rebound. For a more in depth analysis, the fact that dampers are inherently non-linear systems cannot be ignored. Segel, L. and H. Lang [11] presented their study on developing non-linear damper models and found them to be accurate but also computationally expensive. Reybrouck, K. [12] developed a relatively simpler model from previous work which could be used for full vehicle simulations for up to 30 Hz. Although conventional physics based damper models developed have been found to be close to the true behavior of the damper in a controlled environment, the practical feasibility of these models has always been a point of concern due to their high complexity and computationally intensive nature. Semi-active damper modeling has been carried out for a long time now with very well developed Bouc-Wen and Spencer (modified bouc-wen) models [13-15]. The non-linearity of the damper is captured by the Bouc-wen hysteresis model as illustrated in Figure 12. Well established models based on Bouc-Wen hysteresis perform very well to estimate relationship between the force, displacement and velocity of a damper. More often, damper systems are velocity dependent i.e.

the relationship between the force and velocity during compression and rebound dominates the overall dynamics of the damper. Despite development of the discussed non-linear modeling techniques, it is common practice to develop simple algebraic damper models which ignore hysteresis while still maintaining the general trend of the force-velocity relationship. These models work well for low-medium range frequency response and becomes inaccurate as the operation move towards higher frequencies.

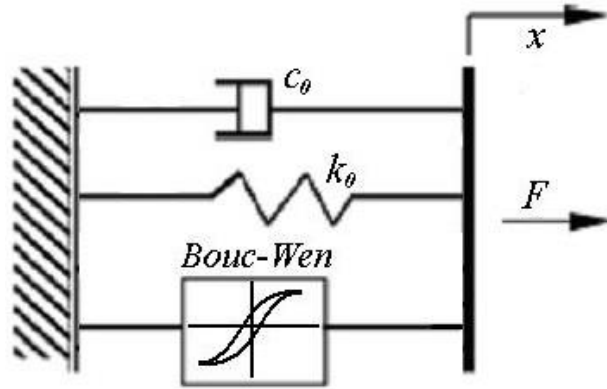


Figure 12: Schematic representation for MR damper modeling

Used under Fair Use 2017 [13]

For an EH semi-active damper like the one used for this study, a simple damper model can be provided to evaluate damper force with varying velocity. The characteristics can be approximated assuming damping force (F_d) dependence on velocity (\dot{x}) through the damping coefficient (c). The friction force of the damper, sometimes also called the ‘breakaway’ force, (F_0) can also be used to express the overall damping force. The damping coefficient itself is a function of voltage (V) and positive gain characteristic (γ). c_{min} and c_{max} are the minimum and maximum damping force the semi-active damper can provide.

$$F_d(\dot{x}, V) = c(\gamma, V)\dot{x} + F_0 \mathbf{sgn}(\dot{x}) \quad (1)$$

$$c(\gamma, V) = \begin{cases} \frac{\gamma}{V} + c_{min} & ; V \neq 0 \\ c_{max} & ; V = 0 \end{cases} \quad (2)$$

$$c_{min} \leq c \leq c_{max} \quad ; \quad 0 \leq V \leq V_{max} \quad (3)$$

Although, multiple parametric and empirical damper models have been discussed in literature since early 1930, relatively new techniques such as using artificial neural networks for damper modeling have been the focus of study which can provide accurate non-linear models while still being computationally inexpensive. This study focuses on a similar approach to model an EH damper.

1.4 Motivation

Evaluation of vehicle performance for ride comfort, handling and safety can be carried out in two major ways; (i) testing on the track or controlled environment using vehicle prototypes (ii) developing accurate models to carry out vehicle simulations. Damper behavior plays a very important role to achieve the desired vehicle performance and more often damper tuning is based on trial and error methods. As discussed in the previous sections, literature review shows extensive research has been carried out in developing models which can represent the true dynamics of a damper yet the conventional methods do not provide a model which is computationally inexpensive and hence easy to use in a real-time simulation, SIL or HIL setups. Therefore, the motivation behind this thesis was to explore a modeling technique to develop a damper model which would be computationally less demanding and would be able to encompass its non-linear behavior for full vehicle simulations.

1.5 Objective of Thesis

For this study, a semi-active damper was fabricated and was used to develop a damper model to be used in further simulations. Therefore, for the scope of this thesis the objectives were set as follows:

- Develop and validate a damper model for an in-house modified semi active damper using artificial neural networks. Secondary objectives were to exploring multiple training algorithms and architectures for efficient model development.
- Develop a modified quarter-car simulation model integrated with the ANN damper model
- Develop a SIL setup using CarSim-Simulink interface to carry out full vehicle simulations
- Evaluate the feasibility and possible effects of using the ANN model in real time vehicle simulations using the quarter car model and CarSim-Simulink SIL setup

1.6 Thesis Outline

The methodology used and layout of the thesis has been summarized into six chapters which have been briefly described as below

Chapter 1 presents a brief introduction to the vehicle suspension system and the categories in which it is generally divided into. Further, semi-active dampers and their types have been discussed with benefits and limitations of each briefly highlighted. Next, a concise literature review on damper modeling has been carried out to focus on the need for accurate damper models. The chapter concludes by stating the motivation, objectives and outline of this thesis.

Chapter 2 introduces artificial neural networks as a technique to model a system. It includes a comprehensive review of the types of neural networks and the argument for using the feed forward MLP network for this study. The chapter also discusses and illustrates the structure of a neural network and its training procedure. Next, three common training algorithms used for error minimization for the network output have been discussed in reasonable detail followed by a brief discussion on advantages and limitations of using the technique. Finally, a concise overview of the MATLAB neural network toolbox has been presented.

Chapter 3 describes the semi-active damper fabricated at CenTiRe and used for this study. Further, the testing rig including a shock dynamometer, damper controller and data acquisition system have been discussed. Experiment repeatability and temperature variation test have been carried out and results analyzed as a part of system robustness check. Lastly, the damper testing plan and the corresponding results obtained after data acquisition have been illustrated.

Chapter 4 starts with a literature review of various architectures proposed to model non-linear dampers using neural networks. After considering the benefits and limitations of the various architectures, a feedforward MLP based architecture with three inputs, thirty hidden layer neurons and one output is proposed. Finally, the trained neural network is validated for prediction accuracy and a summary of the modeling approach has been laid out.

Chapter 5 further expands on the developed ANN damper model by integrating it into a modified

quarter car model as well as a CarSim model. The quarter car simulations have been carried out to check damper model response to impulse, sine-sweep and rough road input. CarSim-Simulink interface has been used to use the developed damper model for full vehicle simulations. Standard ride and handling tests have been carried out and results have been compared to baseline lookup-table based damper models.

Chapter 6 concludes with the reiteration of the need to carry out this study. The key takeaways from work carried out has been summarized by discussing results from each chapter. The study concludes with an outline of the possible future work that can be carried out using the developed damper model and simulation results.

2 ARTIFICIAL NEURAL NETWORKS

2.1 Introduction

Artificial neural systems or neural networks are physically cellular systems which can acquire, store and utilize experimental knowledge [16]. Neural networks are inspired by the way human brains and nervous systems process and store information. They have been studied from as early as 1943 when McCulloch, W. S. et al [17] described ANNs as adaptive nonlinear information processing systems consisting of multiple processing units (neurons) that could self-adapt, self-organize and learn real time. In general, artificial neural networks consist of neurons which are interconnected to each other and work together to solve a given problem. More recently, Laudani, A., et al. [18] described neural networks as a tool for nonlinear mapping of a generic n -dimensional nonlinear function. Ding, S., et al. [19] suggest each neuron is a transfer function which is generally multi input and single output. The number of neurons, the weight associated with each connection and the activation function of each layer defines the network behavior. This activation function is usually as threshold/squashing function. Using experimental data ANNs can be trained to achieve generalizations and extract complex non-linear relationships between the given inputs and outputs.

Neural networks learn or train by iteratively changing the connection weights. The learning process can be carried out in three basic ways: supervised learning, unsupervised learning and reinforcement learning [19]. Wilamowski, B. M. [20] discussed in detail the different learning methods of neural networks including supervised and unsupervised learning with illustrations and examples. Neural networks can also be categorized as Feedforward Neural Networks (FNN), Recurrent Neural Networks (RNN) and Fully Connected Cascade (FCC). In an FNN, the network architecture consists of subsequent layers, each consisting of neurons which are connected to the neurons of the previous and next layer while neurons in the same layers are not connected to each other. Parallel processing of inputs in such a setup is therefore layer dependent but neuron independent. RNNs consist of additional backward connections or time delayed outputs fed back into the network as inputs to capture time varying dynamics of a system [21]. RNNs can be used to model a complex temporal dependent system but are also more difficult to train and implement on line [22]. They can also sometimes make the training and prediction process slower. For this study, a review of different strategies of modeling a damper using both feedforward as well as

recurrent neural networks has been done in the beginning of Chapter 4. Figure 13 shows the flow of information from input to output layer in typical feedforward and recurrent neural networks.

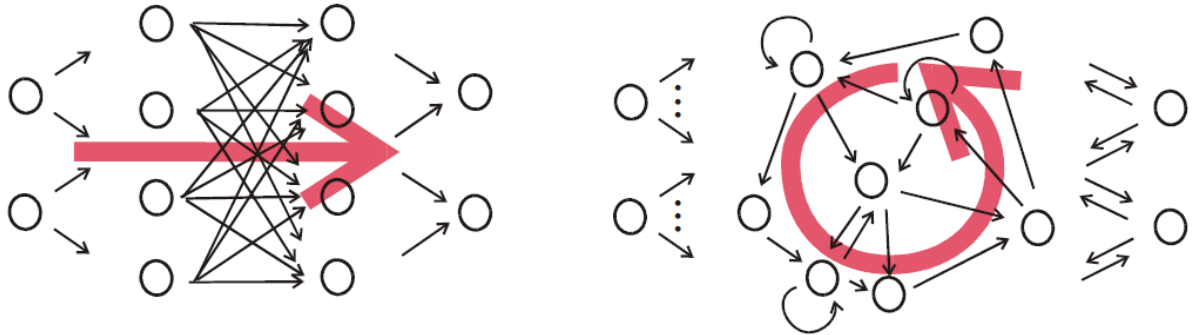


Figure 13: Typical feedforward network (left) and a recurrent network (right)

Used under Fair Use 2017 [21]

Neural networks may also be classified as Multi-Layer Perceptron (MLP) or Radial Basis Function (RBF). MLP are supervised feedforward neural networks trained with the standard back propagation algorithm and are widely used for function fitting and pattern recognition. RBF networks use a Gaussian function to model the non-linearity between the inputs and outputs. It is important to determine a suitable center for the Gaussian. They can be implemented to carry out unsupervised learning [23]. In this study an MLP based feedforward neural network has been developed and discussed in detail in Chapter 4.

2.2 Training of a neural network

A typical neural network structure consists of an input layer, hidden layers and an output layer. For highly complex systems more than one hidden layers can be used but for typical implantations, one hidden layer with adequate number of neurons is usually enough. As discussed before, each layer consists of neurons which take data from one or more inputs and compute an output. The output is computed using an activation function. Table 1 shows the most commonly used activation functions. In this study, the developed ANN uses a sigmoidal activation function for the hidden layer and a linear activation function for the output layer. The neurons are connected to each other by weights that change their value iteratively during the training process. Equation (4) and Equation (5) define the relationship between signals $X_0, X_1, X_2 \dots X_n$ being inputted to a neuron j

and its output Y_j where $W_{j0}, W_{j1}, W_{j3} \dots W_{jn}$ are respective weights associated with neuron j . I_j is the linear combiner output and f is the activation function [24]. Figure 14 shows the architecture represented by these equations. A bias is also added to the input of each neuron making the net input to the neuron $INet_j$ as defined in Equation (6) and illustrated in Figure 15.

$$I_j = \sum_{i=0}^n W_{ji} X_i \quad (4)$$

$$Y_j = f(I_j) \quad (5)$$

$$INet_j = W_{ji} X_i + b \quad (6)$$

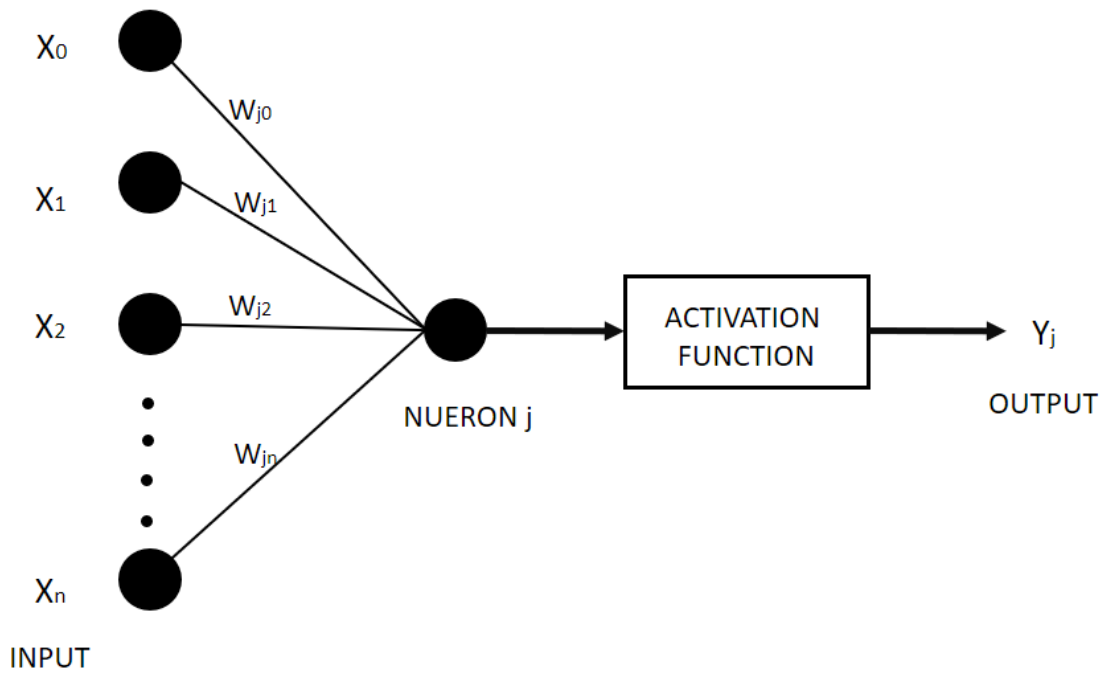


Figure 14: Single Neuron Input and Output Architecture

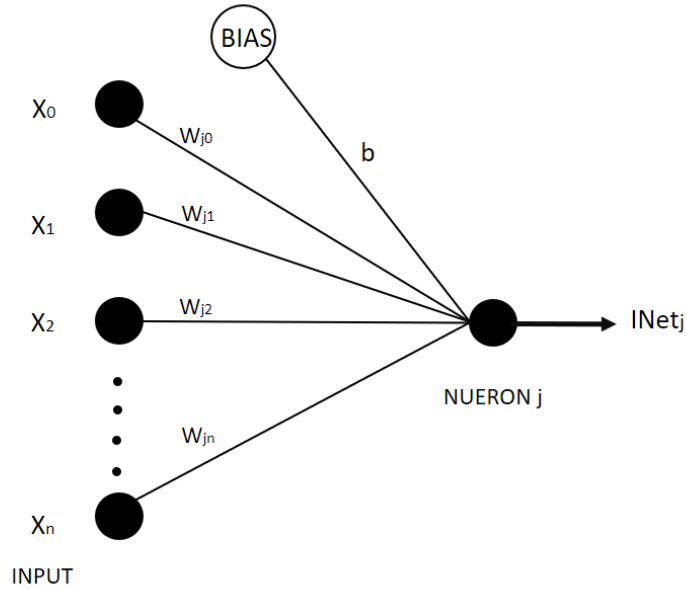


Figure 15: Net Input to Neuron with bias

Table 1: Typical Analytic Activation Functions

S. No	Activation Function	Expression
1	Threshold	$f(x) = \begin{cases} a, & x \geq 0 \\ b, & x < 0 \end{cases}$
2	Linear	$f(x) = \beta x$
3	Sigmoidal	$f(x) = \frac{1}{1 + e^{-x}}$

For a feedforward network when the training is initiated, connections between all neurons are assigned random values. The inputs are then passed through the network and an output is calculated. In the case of supervised learning this output is then compared to the target output and the error is calculated. A backpropagation learning algorithm is used to minimize the error by modifying the connection weights. Essentially the algorithm calculates the effect of changing each weight on the final error. Riedmiller, M. and H. Braun [25] expressed this mathematically as shown in Equation (7) where E is the error function.

$$\frac{\partial E}{\partial w_{ij}} = \frac{\partial E}{\partial X_i} \frac{\partial X_i}{\partial net_i} \frac{\partial net_i}{\partial w_{ij}} \quad (7)$$

Next, using simple gradient descent, the error function is minimized as shown in Equation (8) where $w_{ij}(t)$ is the weight coefficient in step t from neuron i to neuron j and ϵ is the learning coefficient [25].

$$w_{ij}(t + 1) = w_{ij}(t) - \epsilon \frac{\partial E}{\partial w_{ij}}(t) \quad (8)$$

The training continues until the error reaches a desired minimum. Each pass of information from input layer to output layer and back to input layer via back propagation is called an epoch.

2.3 Learning Algorithms

In general, all algorithms work on the same basic principle of minimizing the error by adjusting the weights during the training process. In certain cases, the gradient descent based back propagation algorithm is not the most effective algorithm for error minimization and hence multiple algorithms such as Levenberg – Marquardt, Bayesian Regularization and Scaled Conjugate algorithms have been developed and discussed in the following sections.

2.3.1 Levenberg – Marquardt

A detailed mathematical explanation of the Levenberg-Marquardt [22] algorithm has been discussed by Hagan, M. T. and M. B. Menhaj [26]. The LM algorithm is a trade-off between two separate algorithms, namely the gradient descent algorithm and the Gauss-Newton (GN) method, which have their own advantages and limitations. The LM algorithm essentially switches between these two algorithms at the optimal time and effectively converges to the minimum possible error in the quickest time. Kermani, B. G., et al. [27] further discussed that GN algorithm converges quickly due to its quadratic convergence properties provided the initial set of weights were well chosen. This makes the GN impractical for many applications. On the other hand, the performance of gradient descent algorithm depends less on the initial sets of weights chosen although the error is minimized linearly and is therefore slow. The LM algorithm behaves as a hybrid algorithm which performs well for real world problems. Initially the LM algorithm behaves as a gradient

descent algorithm improving the initial guess of the weights and soon switches to the GN algorithm as it approaches to minimize the error function. It once again switches back to gradient descent after achieving the minimum error to improve accuracy. Equation (9) describes the update rule for GN method where Δw is the weight change suggested by the algorithm, $J(w)$ is the jacobian matrix and $e(w)$ is the error vector.

$$\Delta w = -[J^T(w).J(w)]^{-1}.J^T(w)e(w) \quad (9)$$

The LM algorithm modifies the above equation to give us the new weight change as per Equation (10). Here the value of λ decides whether the algorithm behaves as gradient descent or GN i.e. for high λ values it behaves as scaled gradient and for low λ values it behaves as GN algorithm.

$$\Delta w = -[J^T(w).J(w) + \lambda I]^{-1}.J^T(w)e(w) \quad (10)$$

Lastly the criteria for LM to stop training is same as that for a typical back propagation method.

2.3.2 Bayesian Regularization

Another algorithm to train the network to achieve generalization quickly is the Bayesian Regularization (BR) algorithm. Kumar, P., et al. [28] discussed the fundamentals of the technique. The aim here is to minimize the error function $F = E_d$ where E_d is given by Equation (11) with n being the number of inputs in the training set, t_i being the i^{th} expected output and a_i being the i^{th} output obtained as neural network response.

$$E_d = \sum_{i=1}^n (t_i - a_i)^2 \quad (11)$$

Next for regularization the objective function becomes

$$F = \alpha E_w + \beta E_d \text{ where } E_w = \sum_{i=1}^N w_i^2 \quad (12)$$

Baye's rule of probability is used to determine the optimal value of the objective function parameters, α and β [29].

2.3.3 Scaled Conjugate

A typical backpropagation algorithm adjusts the weight of the network with the objective to obtain the steepest descent. On the other hand, a scaled conjugate algorithm attempts to produce a faster convergence by giving priority to the scaled conjugate direction as compared to the steepest descent direction. Hence for certain networks convergence can be much quicker but can lead to higher prediction errors.

2.4 Advantages & Limitations

Modeling a system using an ANN comes with both its advantages and limitations. The two major advantages of using ANN are the ability to represent the true dynamics of the system using real data while simultaneously by-passing the need to understand the physics of the system in intricate detail. It would not be incorrect to define this approach as a 'Black-Box' model generation where the inputs and outputs of the system are known and the black box has been provided information from test data, as in the case of this study. Another advantage of neural networks is that it is possible to use partially damaged networks which can be utilized to estimate independent behavior of the system. Trained neural networks can be developed using data which is not necessarily fully certain or complete using unsupervised or deep learning techniques.

With its advantages the technique also comes with its set of limitation, the primary one being with the developed 'black-box' which makes it hard to carry out system identification. Typically, the neural network architecture must be defined before it is provided with data for training. This demands some knowledge of the system to be modeled to choose the appropriate inputs and outputs, training algorithm, number of layers and the activation functions. Techniques for constructive neural networks and network pruning have been a topic of study to address the limitation [30].

2.5 MATLAB neural network toolbox

There are multiple commercial packages available which can help develop a neural network model. Java, Python, R and MATLAB are some of the predominant ones being used today. For this study, MATLAB Neural Network Toolbox R2016a was used.

The MATLAB neural network toolbox can be initialized with the `nnstart` command and the neural network start dialog box opens as shown in Figure 16.

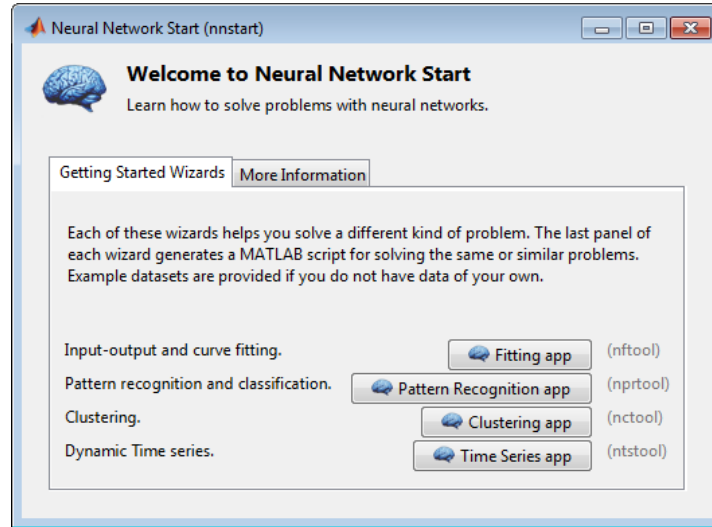


Figure 16: Neural Network Start Dialog Box

The fitting app module was used to model the damper. Input and target vectors need to be made available in the MATLAB workspace for the toolbox and can be selected as shown in Figure 17.

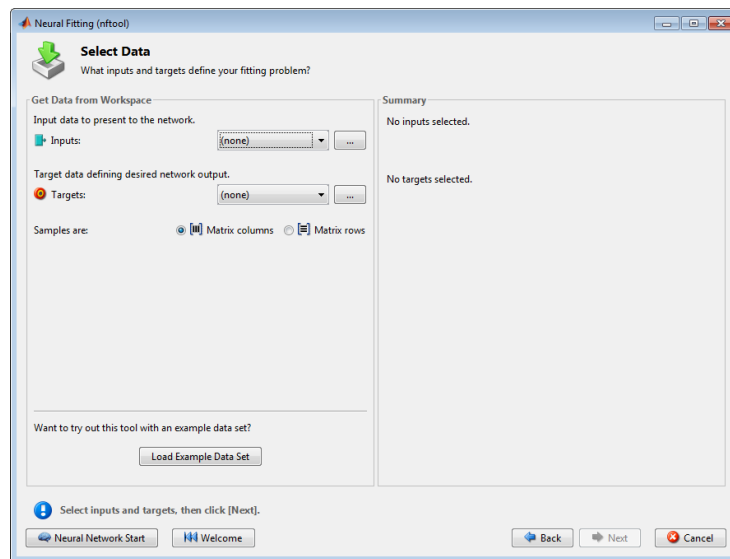


Figure 17: Input and Target data selection from MATLAB workspace

The toolbox by default divides the data randomly into three categories: Training (70%), Validation (15%) and Testing (15%). The training data, as the name suggests, is used to train the network through an iterative process while the weights are adjusted during backpropagation based on the error calculated after each epoch. The validation data is used to determine if the network has achieved the required generalization and decides if the training can be stopped and overfitting be avoided. The testing data is used as an independent measure to evaluate the prediction performance of the trained neural network. It provides a measure of the mean squared error and R- value to assess how well the network has trained. The division of data into training, validation and testing data can be changed as shown in Figure 18.

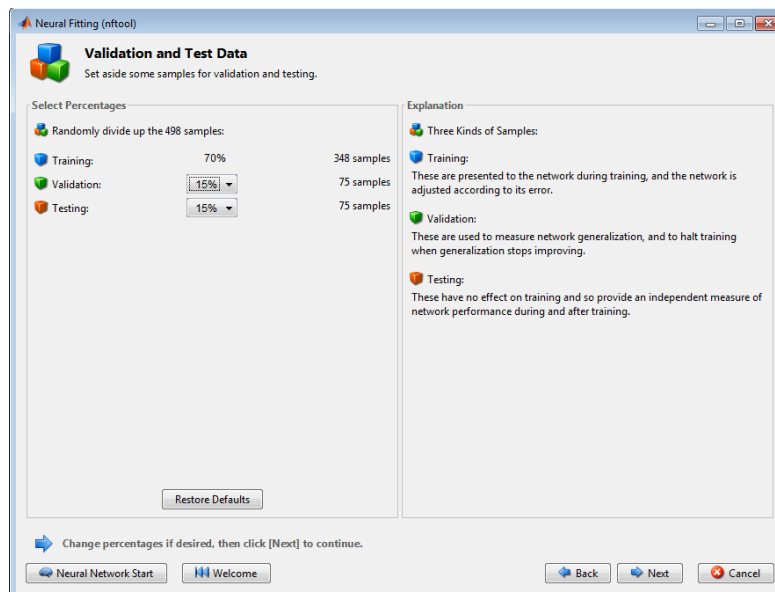


Figure 18: Division of Dataset for Training, Validation and Testing

The toolbox then provides a dialog box to define the network architecture. By default, the toolbox proceeds with a single hidden layer with a sigmoid activation function and a linear activation function for the output layer as shown in Figure 19. For this study a hidden layer with 30 neurons was decided based on literature study and multiple iterations which is discussed in Chapter 4.

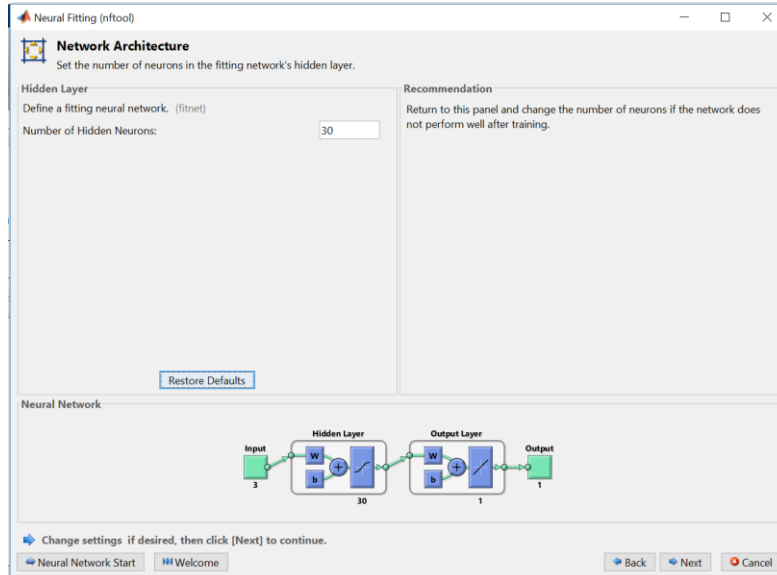


Figure 19: Selection of neurons for network architecture

The network is now ready to be trained and provides an option to choose from the three most commonly used back propagation algorithms already discussed in this chapter. After the training is completed the toolbox provides an option of adjusting the network size if the performance is not as per desired. Finally, multiple options of deploying the neural network through MATLAB scripts or SIMULINK diagrams is presented as shown in Figure 20. For this study, the generated Simulink diagram was used to deploy the trained network to carry out further simulations.

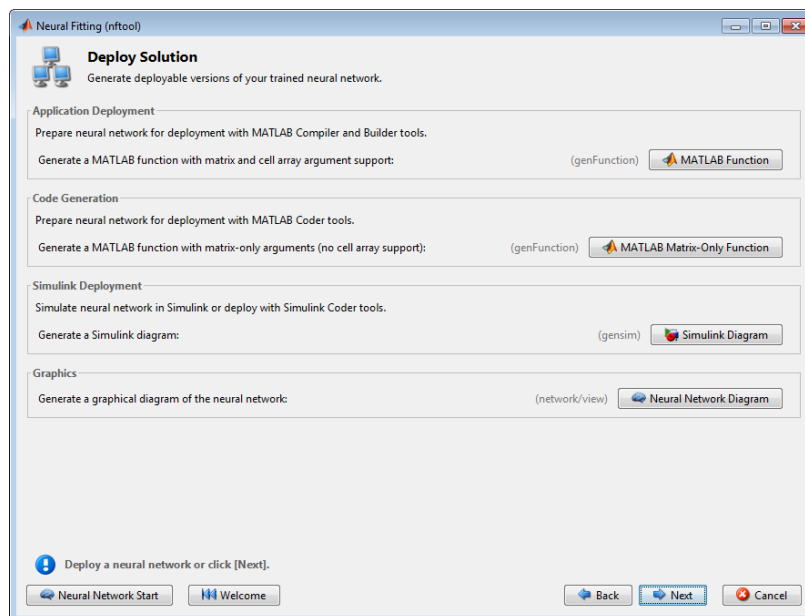


Figure 20: Deploy Neural Network

In general, the neural network toolbox provides an extremely intuitive interface and enough flexibility to develop complex feed forward MLP neural networks.

3 DAMPER FABRICATION, SETUP AND TESTING

To train the NN, a semi active damper was developed in house and was tested on the shock dynamometer. The damper was based on a modified monotube damper which was converted into an external bypass, electro-hydraulic semi active damper. Damper testing was carried out on a shock dynamometer covering frequencies from 0.25 HZ – 3 HZ. This helped capture damper effects on yaw, roll and pitch dynamics of a typical vehicle. For each frequency, damping coefficient was also varied. Finally, the obtained test data was processed in MATLAB for further use.

3.1 Semi Active Damper Setup and Control

A Fox[®] 2.0 monotube shock for a Chevrolet Silverado rear suspension system was specifically chosen due to its compatibility with the current quarter car rig at CenTiRe Lab for future studies. While establishing the design, and fabricating the semi active damper, priority was placed on overall cost, flexibility of control and functionality. As discussed above, it was decided to modify a monotube shock by providing an external bypass from one chamber to the other. The flow rate was controlled using a flow controlling bi-directional solenoid valve. Figure 21 shows the semi-active damper with the solenoid valve. A gas pressure of 200 psi was used for the nitrogen chamber.



Figure 21: Semi Active Damper

Janse van Rensburg et al. [31] focused on modeling the bypass valve for a semi-active damper. It was concluded in the study that due to involvement of fast acting dynamics it was necessary to use valves capable to handle high pressure and flow rates during high speed damper testing. Accordingly, a HydraForce SP10-24 solenoid valve was used as shown in Figure 22. It is a proportional solenoid-operated, 2-way, spool-type, normally closed, providing bi-directional fluid metering. When energized, it allows change in area based on change in voltage/current up to 5V/1.2 A. The valve can withstand pressures up to 3000 psi and allows fluid volumes of up to 7 gpm. The response time for the valve from fully closed to fully open is approximately 40ms, thus acceptable for its use in the semi active damper setup.



Figure 22: HydraForce SP10-24 solenoid valve

A HydraForce EVDR-0101A controller was used to control the current provided to the solenoid valve. The controller was configured using HF-Impulse software tool provided by HydraForce.



Figure 23: HydraForce Controller-0101A

3.2 Testing Setup

An Intercomp 2HP Shock Dynamometer, available at CenTiRe, was used to test the semi active damper. The testing and data collection diagram has been illustrated in Figure 24 and the actual setup is shown in Figure 25.

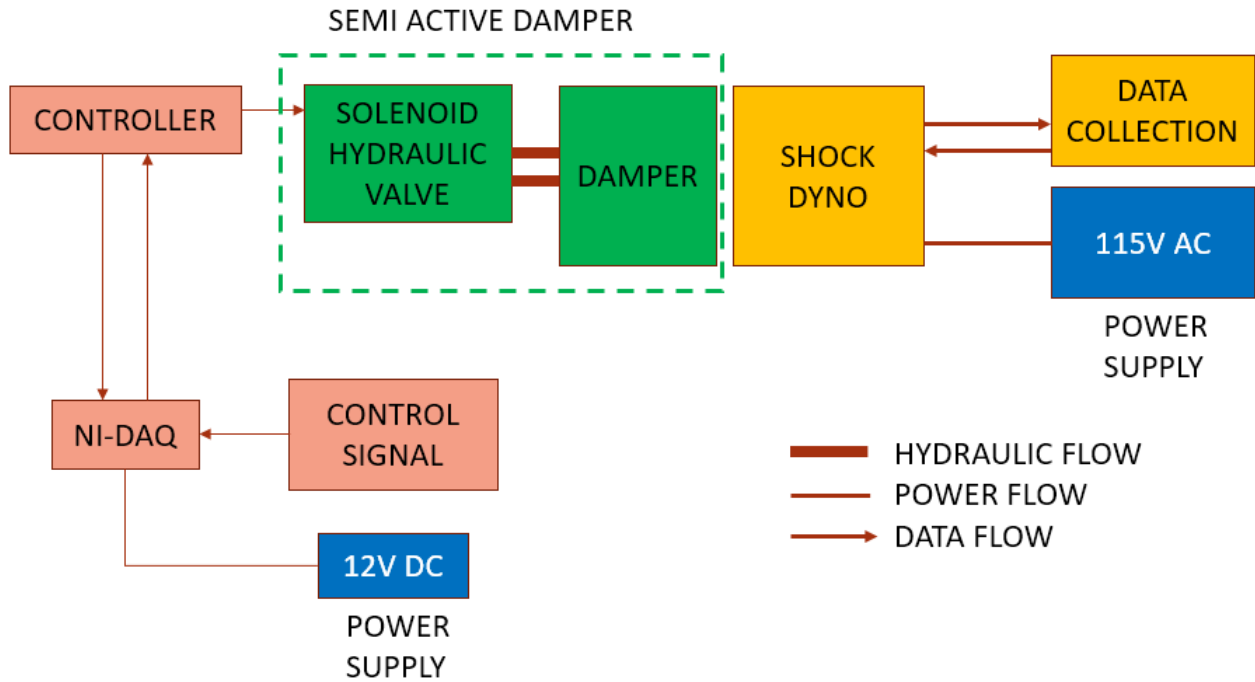


Figure 24: Testing and Data Collection Diagram



Figure 25: Testing and Data collection setup at CentiRe

The shock dynamometer consisted of a load cell to measure forces experienced by the eyelet of the damper. Also, the custom Intercomp software estimated the displacement and velocity values by measuring the RPM of the motor for each test. A text file with 10,000 data points each for force, displacement and velocity was exported for every test run and the obtained data was processed using MATLAB. The EVDR controller was calibrated using the HF-Impulse software such that it took inputs from 0 – 5 volts and provided a current output for the solenoid valve to go from fully closed (0A) to fully open (1.2A) state. Figure 26 shows the software interface where the required inputs were programmed into the controller as per solenoid specifications. A LabVIEW program, as shown in Figure 27 was setup and an NI-DAQ was used to provide the controller the desired input voltage, effectively making it possible to vary the damping in real time.

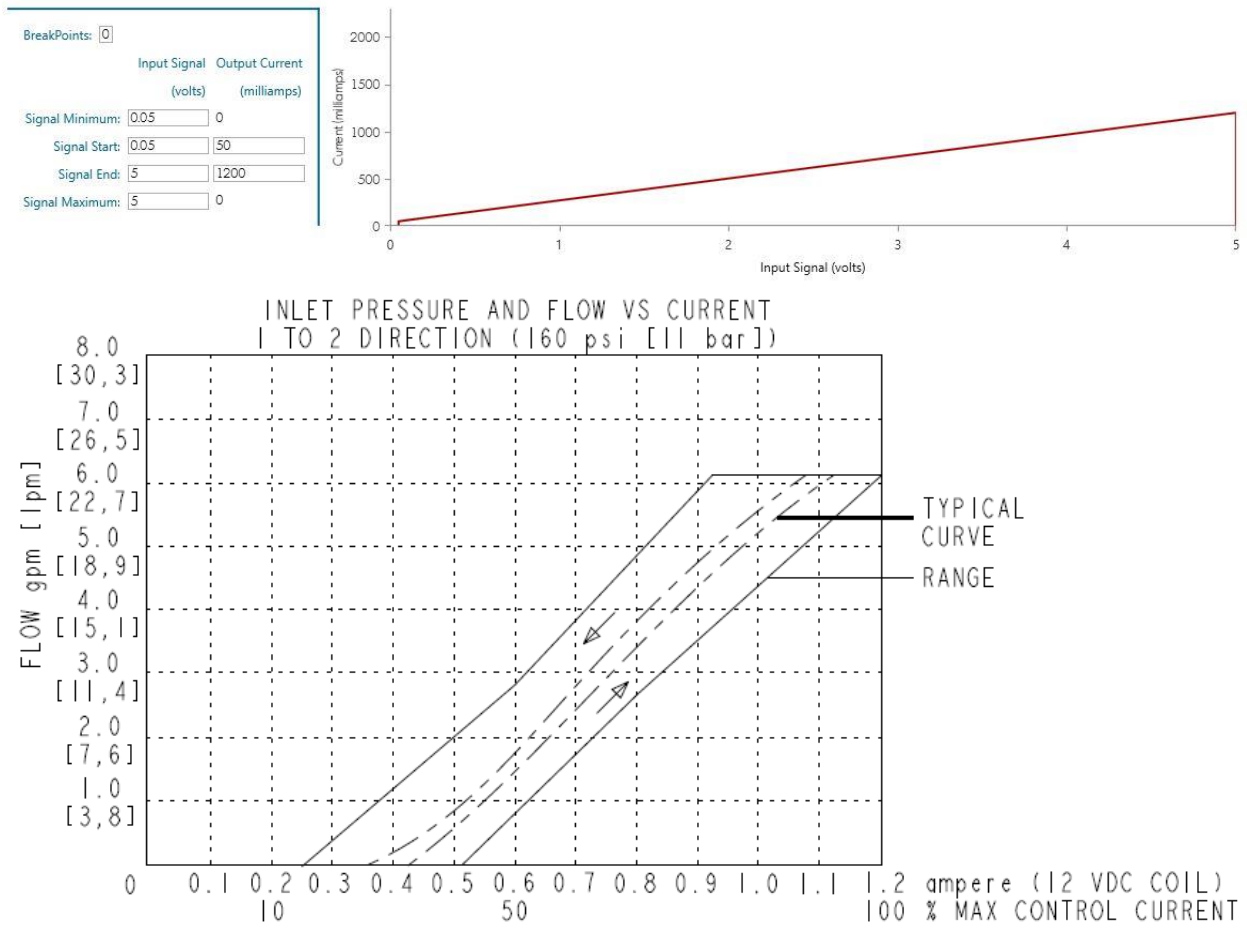


Figure 26: Controller calibration (top) and valve specifications (bottom)

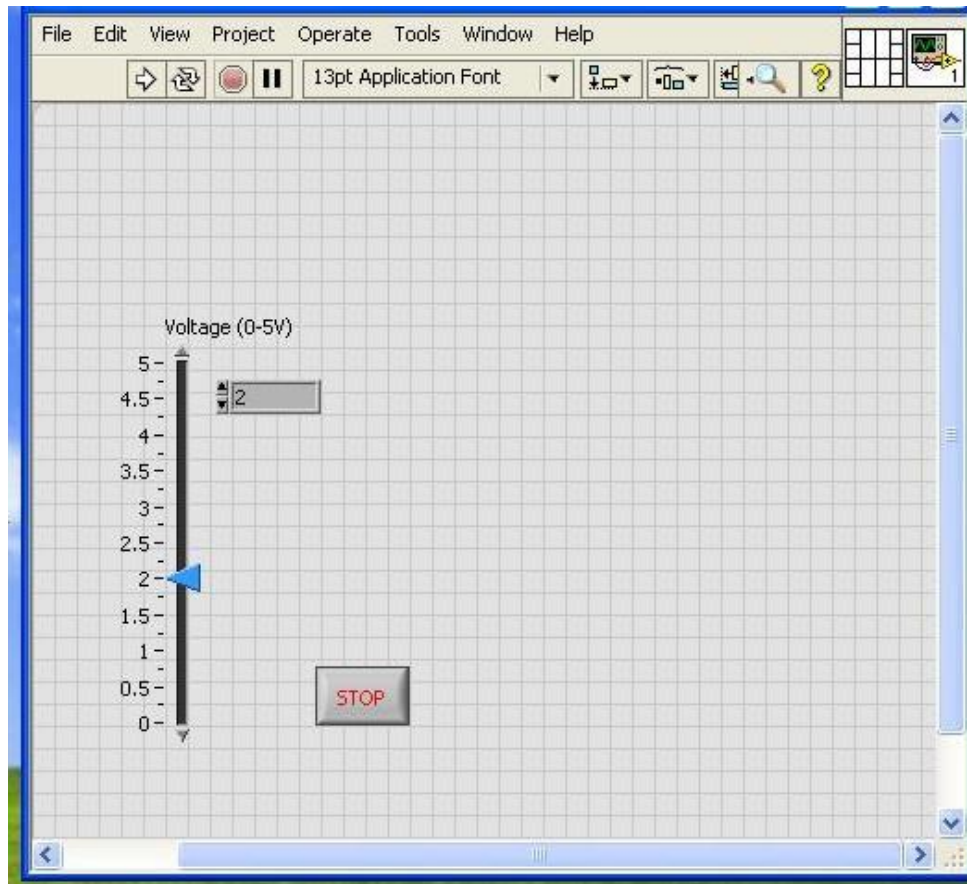


Figure 27: LabVIEW Program for valve control

3.3 Damper Testing and Data Collection

The test setup was used to test the semi active damper under multiple conditions. First, the repeatability of tests for the complete system was checked to establish the robustness of the test setup. Figure 28 shows typical Force vs Displacement curves obtained for different testing frequencies with a sine input with an amplitude of 1 inch. The plots confirmed the test setup had sufficient repeatability.

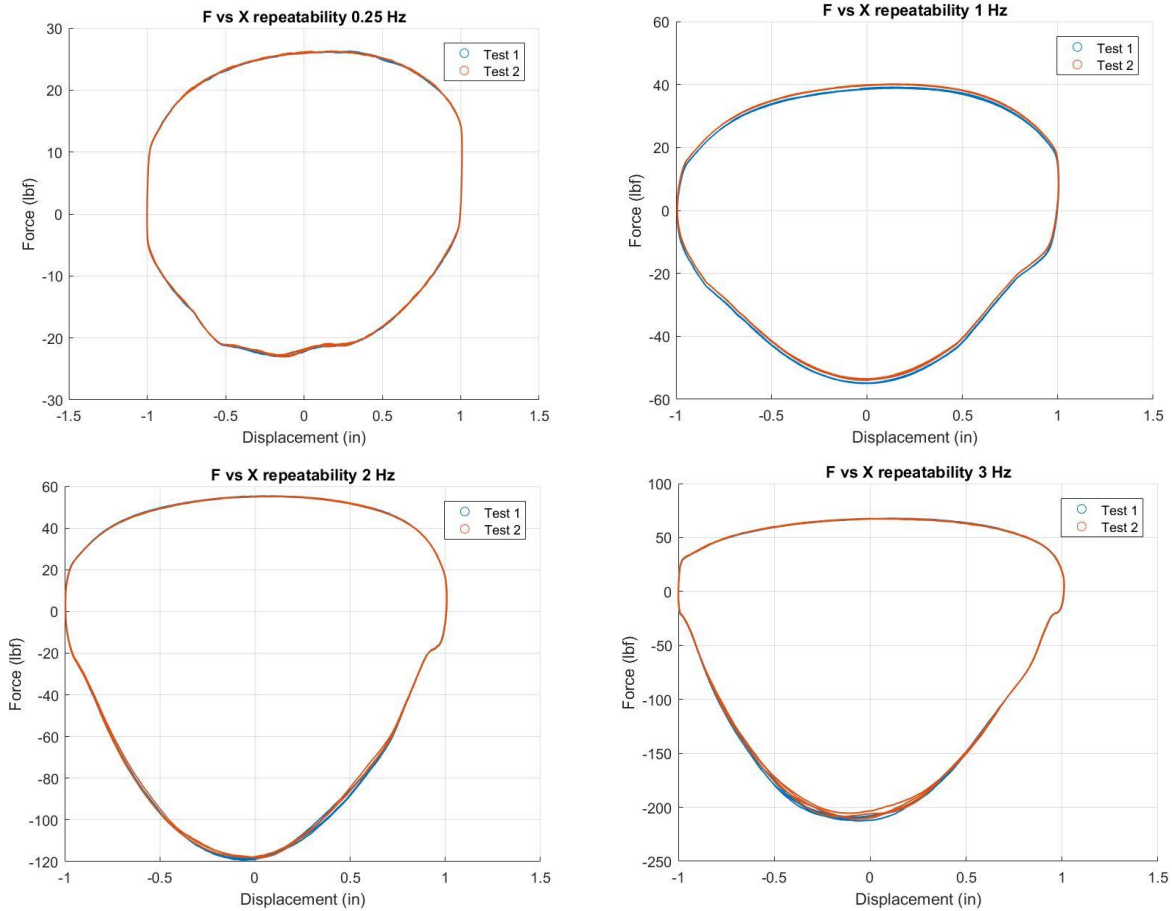


Figure 28: Repeatability Test Results (0.25 Hz-3 Hz)

Next, the effect of temperature variation was studied for the damper by carrying out tests at different damper temperatures (90°F, 100°F, 105°F and 120°F) and at different frequencies. Temperature was monitored by placing a K-Type thermocouple approximately between the two by pass valve ports on the damper body. The Force vs Displacement graphs for the damper for each tested frequency at different temperatures are shown in Figure 29. It was concluded that temperature changes do not have a significant effect on the damper forces (± 5 lbs) if temperature remains in the ballpark operating range. All further testing was carried out at $100 \pm 2^\circ\text{F}$ for consistency.

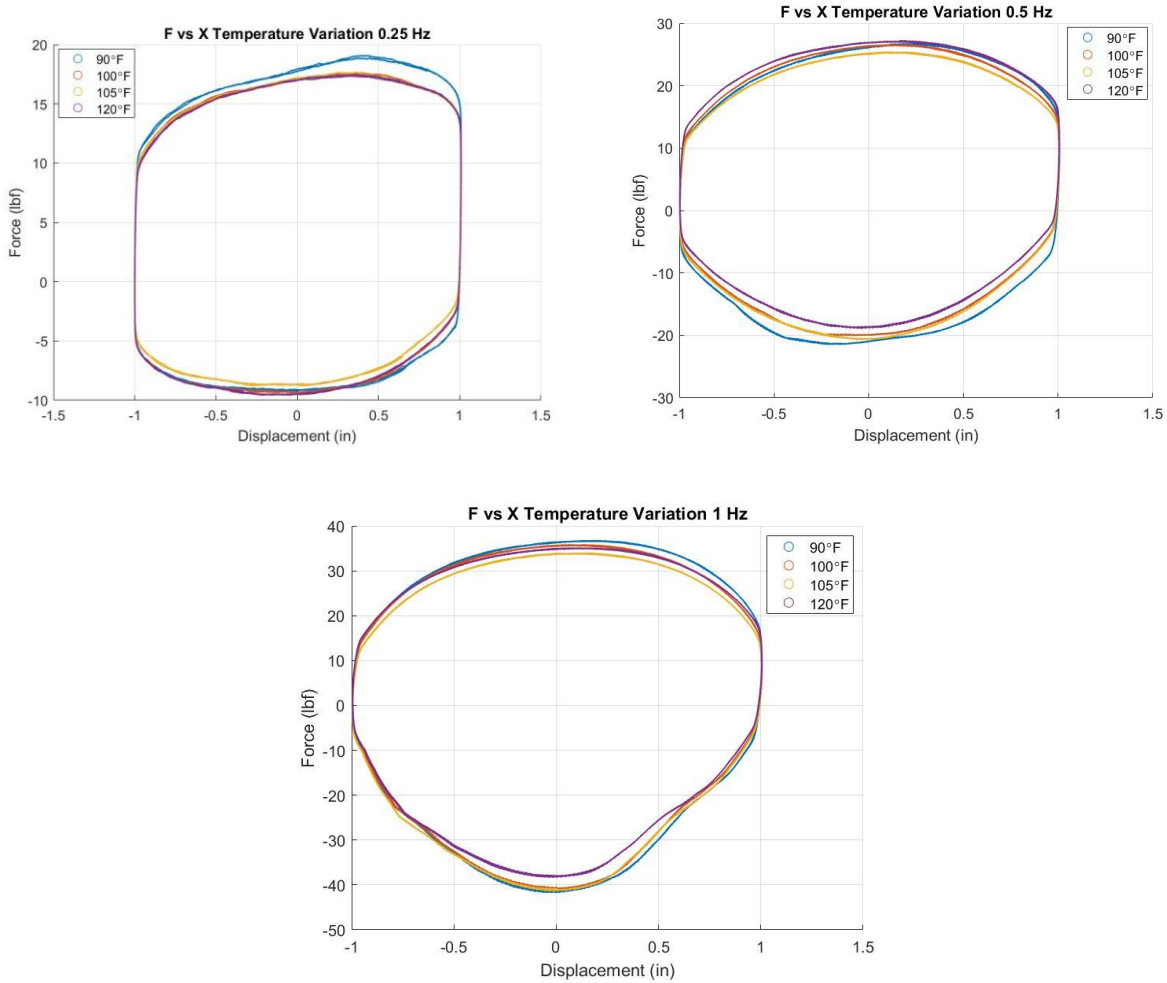


Figure 29: Temperature Variation Test Results (0.25 Hz - 1 Hz)

It was essential to test the damper over its full range of motion to obtain data for both linear and non-linear domain. Table 2 shows the testing plan that was followed to capture damper forces for multiple input frequencies and effective damping coefficients. The test setup ensured voltage change to the controller resulted in change of the bypass ratio of the damper and effectively its damping coefficient. Testing was done for frequencies ranging from 0.25Hz - 3Hz to capture damper behavior that would be exhibited in typical yaw, roll and pitch dynamics of the vehicle. Further, considering the sensitivity of the change in damping with change in the voltage, 15 different voltage values were used to carry out 15 tests at each frequency for which the damper was being tested. A total number of 180 were tests carried out for data collection.

Table 2: Semi Active Damper Testing Plan for 2-inch stroke

Test Number	Damper Temp (°F)	Speed (Inps)	Frequency (Hz)	Voltage to Controller (V)	Corresponding Current (mA)
Test 1 - Test 15	100±2	1	0.25	0, 0.5, 1, 1.25, 1.5, 1.75, 2, 2.25, 2.5, 2.75, 3, 3.5, 4, 4.5, 5	20, 50, 100, 130, 165, 195, 240, 290, 335, 410, 440, 585, 730, 890, 1180
Test 16 - Test 30	100±2	2	0.5	0, 0.5, 1, 1.25, 1.5, 1.75, 2, 2.25, 2.5, 2.75, 3, 3.5, 4, 4.5, 5	20, 50, 100, 130, 165, 195, 240, 290, 335, 410, 440, 585, 730, 890, 1180
Test 31 - Test 45	100±2	3	0.75	0, 0.5, 1, 1.25, 1.5, 1.75, 2, 2.25, 2.5, 2.75, 3, 3.5, 4, 4.5, 5	20, 50, 100, 130, 165, 195, 240, 290, 335, 410, 440, 585, 730, 890, 1180
Test 46 - Test 60	100±2	4	1	0, 0.5, 1, 1.25, 1.5, 1.75, 2, 2.25, 2.5, 2.75, 3, 3.5, 4, 4.5, 5	20, 50, 100, 130, 165, 195, 240, 290, 335, 410, 440, 585, 730, 890, 1180
Test 61 - Test 75	100±2	5	1.25	0, 0.5, 1, 1.25, 1.5, 1.75, 2, 2.25, 2.5, 2.75, 3, 3.5, 4, 4.5, 5	20, 50, 100, 130, 165, 195, 240, 290, 335, 410, 440, 585, 730, 890, 1180
Test 76 - Test 90	100±2	6	1.5	0, 0.5, 1, 1.25, 1.5, 1.75, 2, 2.25, 2.5, 2.75, 3, 3.5, 4, 4.5, 5	20, 50, 100, 130, 165, 195, 240, 290, 335, 410, 440, 585, 730, 890, 1180
Test 91 - Test 105	100±2	7	1.75	0, 0.5, 1, 1.25, 1.5, 1.75, 2, 2.25, 2.5, 2.75, 3, 3.5, 4, 4.5, 5	20, 50, 100, 130, 165, 195, 240, 290, 335, 410, 440, 585, 730, 890, 1180
Test 106 - Test 120	100±2	8	2	0, 0.5, 1, 1.25, 1.5, 1.75, 2, 2.25, 2.5, 2.75, 3, 3.5, 4, 4.5, 5	20, 50, 100, 130, 165, 195, 240, 290, 335, 410, 440, 585, 730, 890, 1180
Test 121 - Test 135	100±2	9	2.25	0, 0.5, 1, 1.25, 1.5, 1.75, 2, 2.25, 2.5, 2.75, 3, 3.5, 4, 4.5, 5	20, 50, 100, 130, 165, 195, 240, 290, 335, 410, 440, 585, 730, 890, 1180
Test 136 - Test 150	100±2	10	2.5	0, 0.5, 1, 1.25, 1.5, 1.75, 2, 2.25, 2.5, 2.75, 3, 3.5, 4, 4.5, 5	20, 50, 100, 130, 165, 195, 240, 290, 335, 410, 440, 585, 730, 890, 1180

Test 151 - Test 165	100±2	11	2.75	0, 0.5, 1, 1.25, 1.5, 1.75, 2, 2.25, 2.5, 2.75, 3, 3.5, 4, 4.5, 5	20, 50, 100, 130, 165, 195, 240, 290, 335, 410, 440, 585, 730, 890, 1180
Test 166 - Test 180	100±2	12	3	0, 0.5, 1, 1.25, 1.5, 1.75, 2, 2.25, 2.5, 2.75, 3, 3.5, 4, 4.5, 5	20, 50, 100, 130, 165, 195, 240, 290, 335, 410, 440, 585, 730, 890, 1180

Data from all tests was collected and processed further in MATLAB for the neural network training or for determining prediction accuracy independently (Discussed in Chapter 4). The collected data agrees with the expected behavior from a semi active damper. With increase in frequency, the damper forces increase. The trend shows the damper being tested has been tuned for slow rebound recovery i.e. the damper will be softer in compression as compared to when it is experiencing rebound/jounce. Figure 30, Figure 31, Figure 32 and Figure 33 show the typical force-displacement and force-velocity behavior the damper exhibited at multiple frequencies and varying voltage. For brevity, data for frequencies of 0.25, 1 Hz, 2 Hz and 3 Hz has been shown out of all the frequencies for which it was tested. Also, to maintain legibility, changing behavior of the semi active damper has been demonstrated by plotting data for 0V, 1V, 1.5V, 1.75V, 2V, 2.5V, 3V and 5V out of the voltages that were used for testing. However, data from all tests at different frequencies and voltages shown in Table 2 was used to develop the neural network damper model.

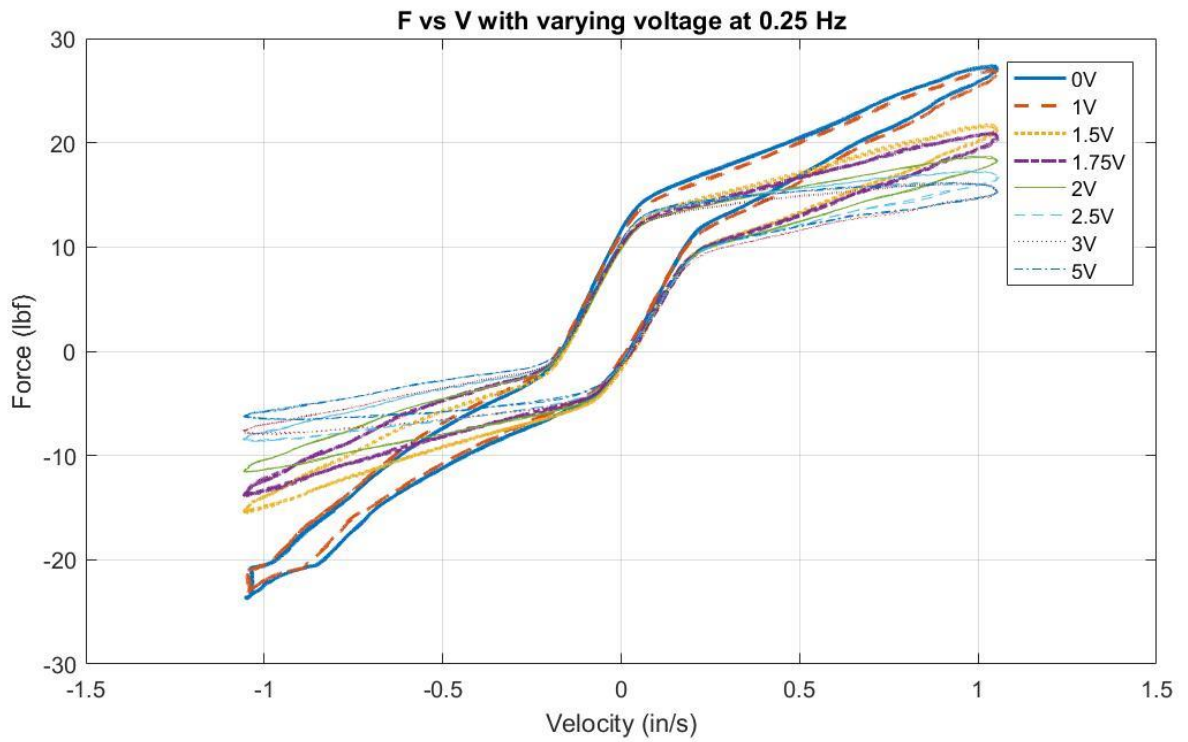
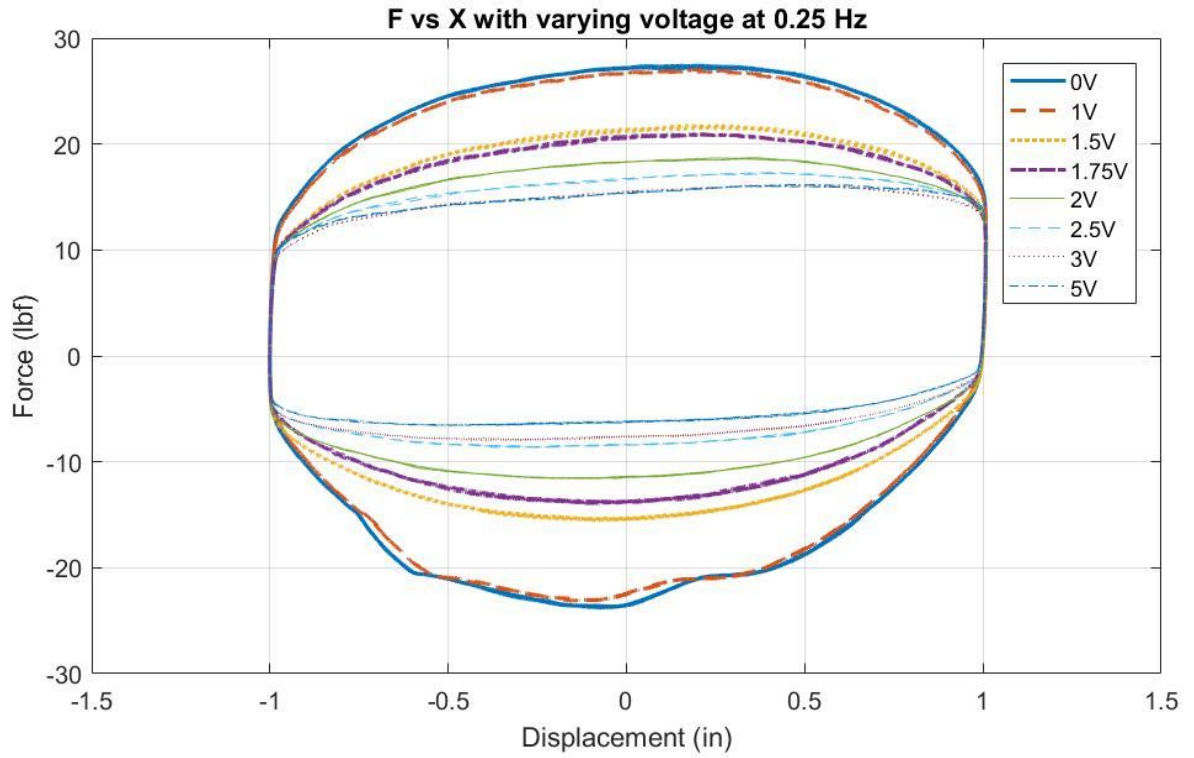


Figure 30: Damper Characteristics at 0.25 Hz - F vs X (Top) & F vs V (Bottom)

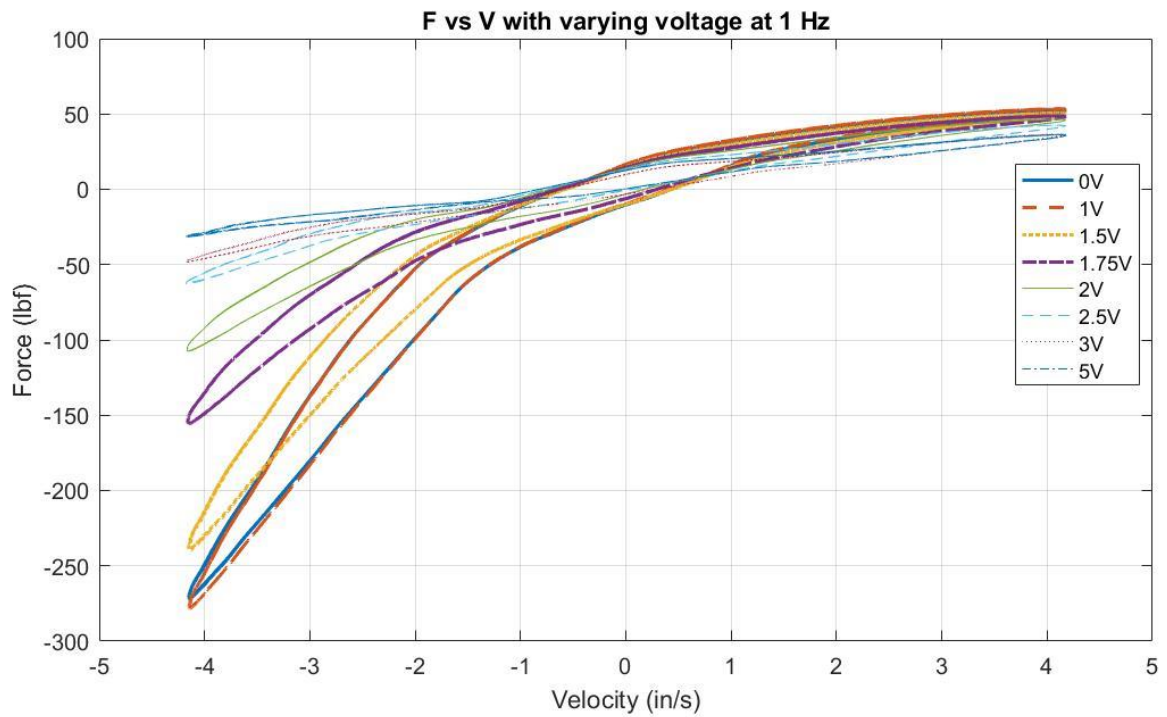
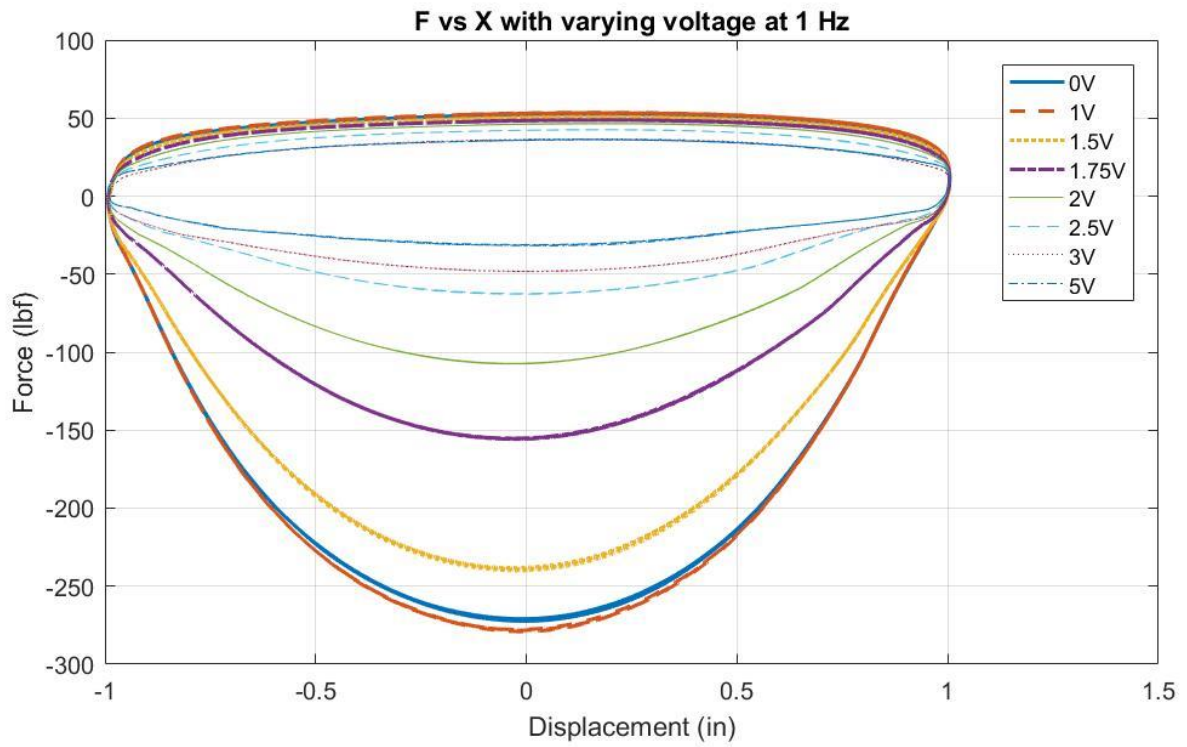


Figure 31: Damper Characteristics at 1 Hz - *F vs X (Top) & F vs V (Bottom)*

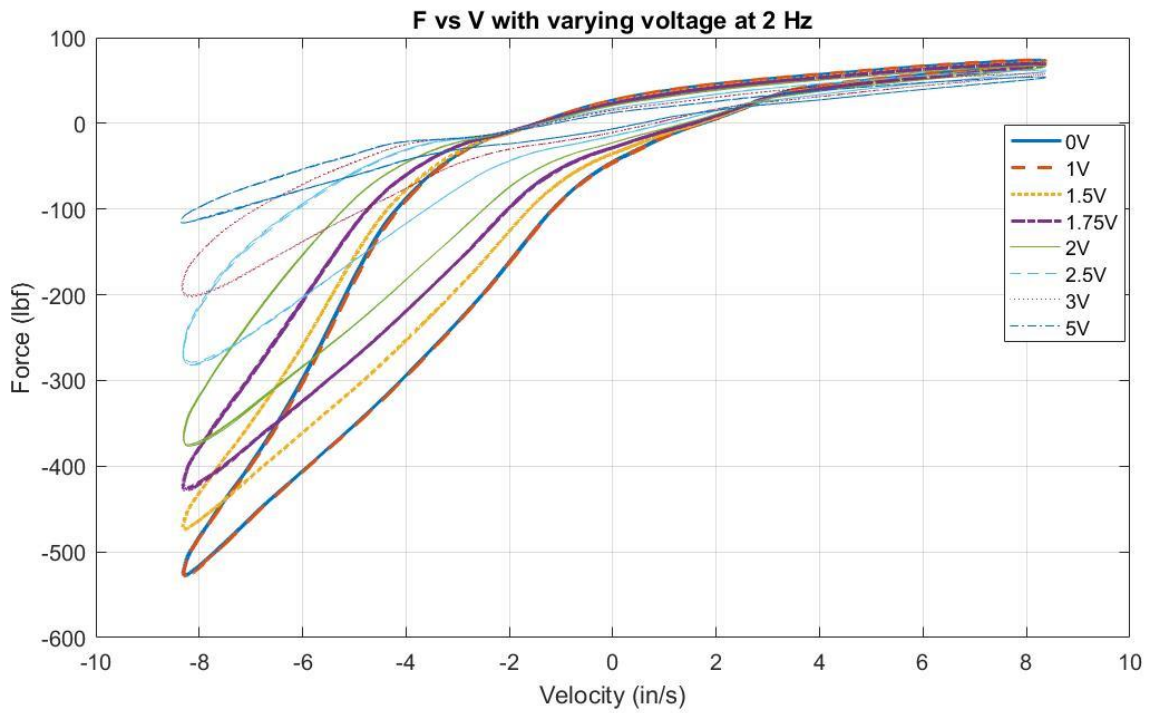
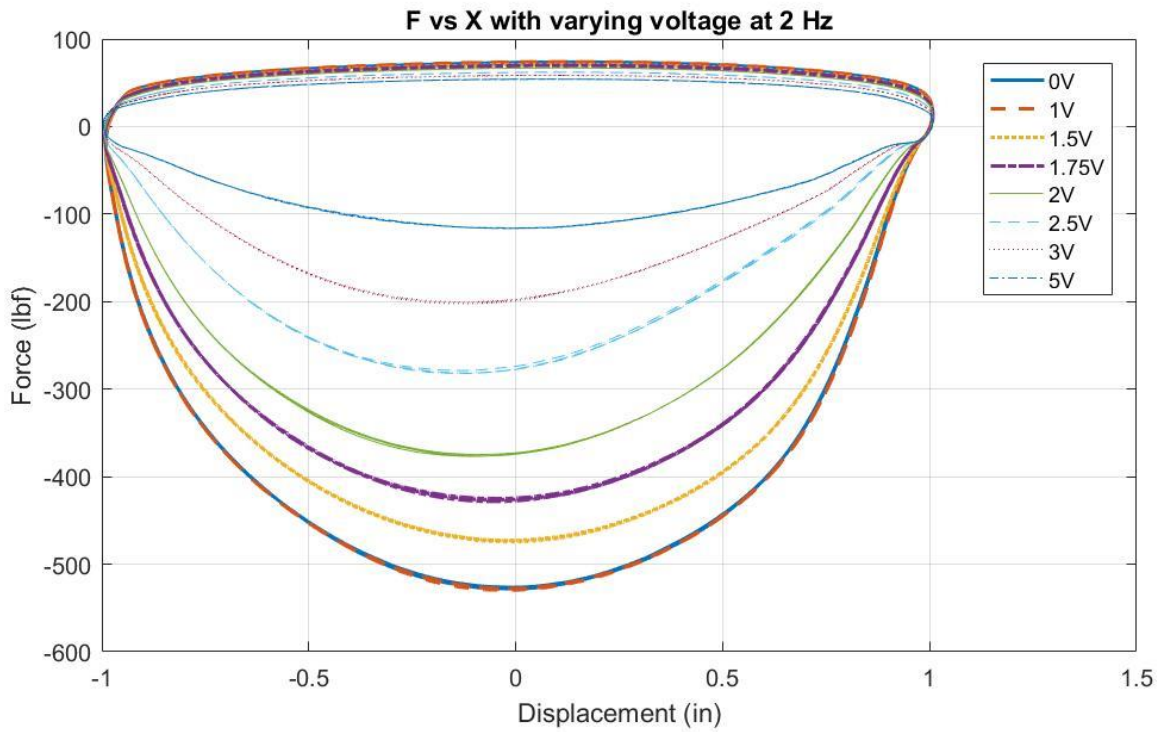


Figure 32: Damper Characteristics at 2 Hz - F vs X (Top) & F vs V (Bottom)

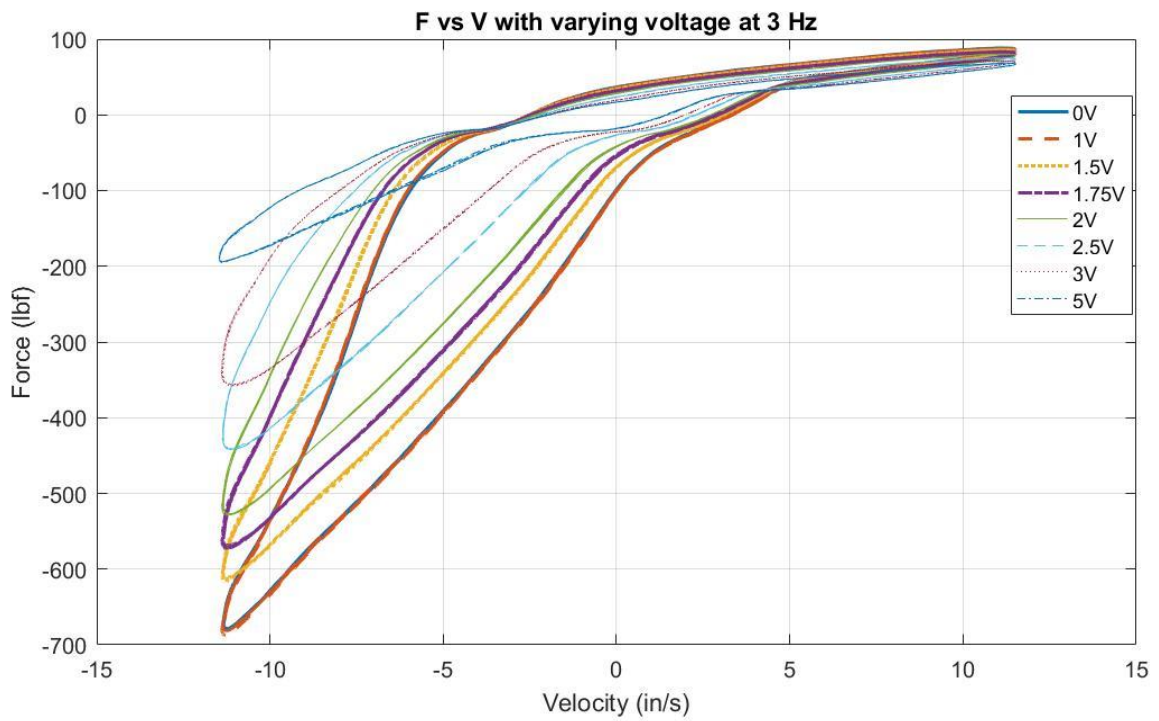
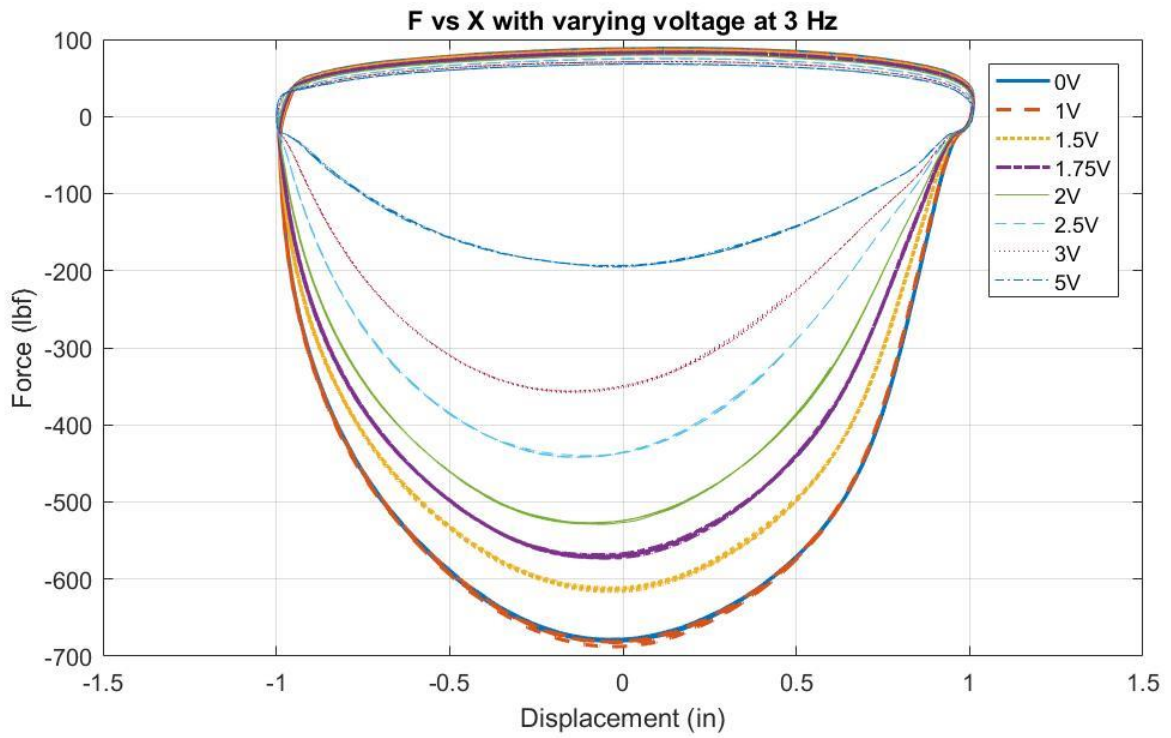


Figure 33: Damper Characteristics at 3 Hz - *F vs X (Top) & F vs V (Bottom)*

4 ARCHITECTURE, TRAINING AND EVALUATION OF ANN MODEL

4.1 Introduction

Gao, B., et al. [32] modeled a strut using neural networks and used displacement and velocity as inputs to the network and obtained force as output. Also, the hidden layer consisted of 30 neurons for the required flexibility while avoiding overfitting. Khalid, M., et al [33] carried out dynamic neural network modeling of MR dampers using displacement, velocity and supplied voltage as inputs to obtain a single output of force. Also, it was highlighted that using a tapped delay recurrent neural network could help develop a more accurate ANN, if the network developed using conventional feedforward training did not perform well. Although, using an RNN would lead to slower training as well as performance. Priyandoko, G., et al [34] developed a back propagation ANN for an MR damper with inputs as current, displacement and velocity and output as damper force. Chang, C.-C., et al [35] evaluated a feed forward multilayer perceptron (MLP) network which was developed using 6 inputs and 1 output. The displacement and velocity input were for real time and previous time step values and the force inputs were from the previous two time steps. Ekkachai, K., et al. [36] introduced a more novel methodology to model non linearity in dampers by using a feed forward neural network to first develop a hysteresis model and then further use the output of that model to predict the damper values. The inputs to the hysteresis model were velocity, acceleration and value from the elementary hysteresis model (EHM). Inputs to the gain function which was responsible to predict the damper force were the output of the hysteresis model and the current supplied. It was concluded that such an approach had an advantage of not needing to provide past information to the network in real time. Burnett, M., et al., [37] also evaluated a neural network model which was developed using displacement, velocity and acceleration as inputs to give a damper force output. It was emphasized that the damper did not need previous values of the output to be fed into the network for future predictions and hence was easier to implement.

For the neural network developed in this study, data was collected from the tests carried out on the semi active damper and was imported into MATLAB. Additional conditioning of the acceleration signal was also carried out to remove noise. The data was restructured for use in the MATLAB Neural Network Toolbox with the inputs of the ANN being velocity, acceleration and voltage and

the output being the force. Supervised learning of the network was done. Data collected during tests at all frequencies corresponding to 2.25V was separated from the set of data used for network training. It was done so to achieve an independent set of data, unseen by the network, for evaluating the prediction accuracy of the developed ANN model at the same voltage input. Finally, the performance of all three available training algorithms in the toolbox was evaluated. The ANN trained using ‘Levenberg- Marquardt’ algorithm was selected for further study. Figure 34 shows the framework for the ANN that was developed for damper force prediction.

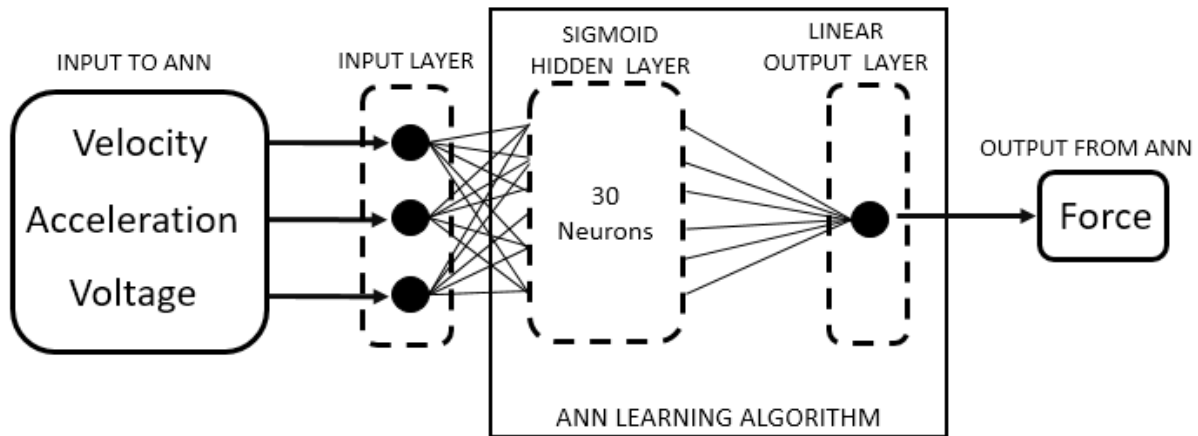


Figure 34: Developed ANN Architecture

4.2 Data Processing for ANN Training

The Intercomp software provided a text file for each test run consisting of 10000 data points of force, displacement and velocity the damper experienced for the given sine input. The data for all tests was imported into MATLAB and processed for use in the Neural Network Toolbox. Most dampers are velocity sensitive and hence it was decided to use velocity as one of the inputs for the desired network. The second input was chosen to be acceleration as it could provide the network information about how fast or slow the dynamics of the damper were changing and hence output expected forces accordingly. The acceleration signal was extracted from the available displacement and velocity signals from each test. The shock dynamometer samples the data at 5000 Hz. Accordingly using kinematics, the acceleration signal was calculated for every instant. The noise in the acceleration signal was filtered using a moving average filter in MATLAB before using it to train the neural network.

4.3 ANN Training and Validation

The toolbox gives an option of choosing among 4 available wizards depending upon the type of problem needed to be solved by the neural network. The fitting app wizard was selected as it could solve our problem of developing a non-linear relationship between inputs and targets using the available test data. The dataset was randomly divided into three subsets: Training (70%), Validation (15%) and Testing (15%). As per the description the training dataset is used to carry out supervised training and develop a feed forward neural network. The validation dataset is used to stop the learning algorithm when the generalization stops improving. The testing dataset is used to provide an independent measure of how the network performs after the training. The inputs to the model were velocity, acceleration and voltage with the output as damper force. After training, using multiple networks with varying number of neurons in the hidden layers and comparing their mean squared error (MSE) values for a minimum, the network which was finally used for further simulations was trained using 30 neurons in the hidden layer. All three algorithms available in the toolbox were used and performance was compared by using the trained networks for predicting outputs for an independent set of inputs. Table 3 shows the performance of each algorithm. Accordingly, the network trained using Levenberg-Marquardt algorithm was selected for further simulations due to lowest MSE.

Table 3: Comparison of Learning Algorithms

Learning Algorithm	Normalized RMSE ^a	Training Time (minutes)
Levenberg - Marquardt	0.0339	106
Bayesian Regularization	0.0422	111
Scaled Conjugate	0.112	89

^a Root Mean Squared error divided by max-min range of its dataset

The distribution of error for the networked trained using the selected algorithm is shown in Figure 35. For a well-trained network the errors should be as close to zero as possible which in the figure is represented by the ‘zero error’ line. As can be observed, most errors for the ANN are close to zero. Hence the number of neurons chosen are enough.

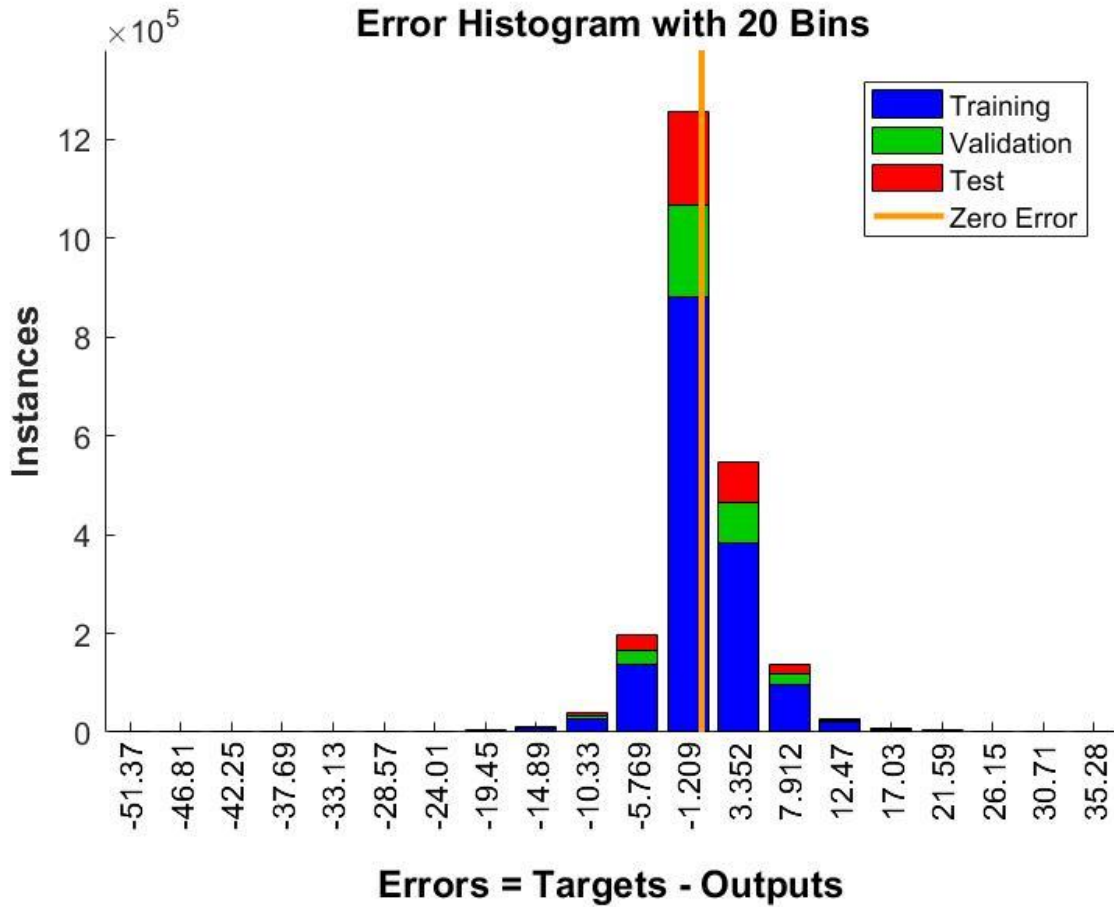


Figure 35: Error Distribution for Damper Force

For further validation, the developed network was used to predict damper values for an independent set of inputs corresponding to 2.25V. The predicted output values were compared to the actual values recorded during the testing at 0.25 Hz, 1 Hz, 2Hz and 3 Hz. Figure 36, Figure 37, Figure 38 and Figure 39 show the performance of the network for different frequencies. Validation can also be carried out by varying voltages at the same frequency, but for the sake of brevity it was left for another complementary study.

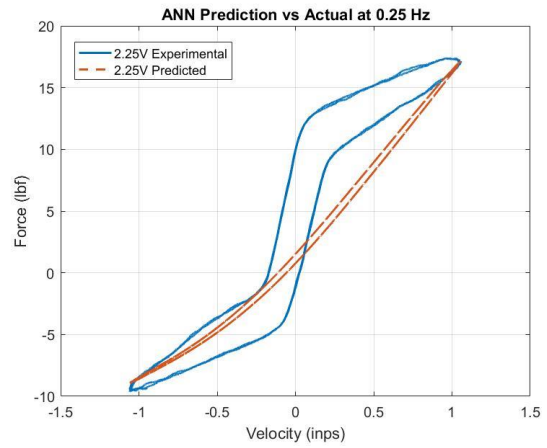
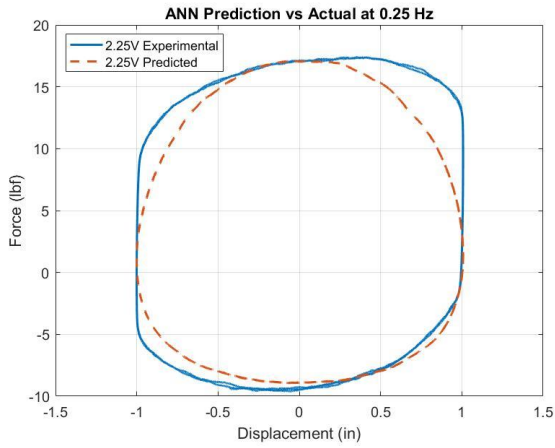


Figure 36: Predicted vs Actual Force at 0.25 Hz

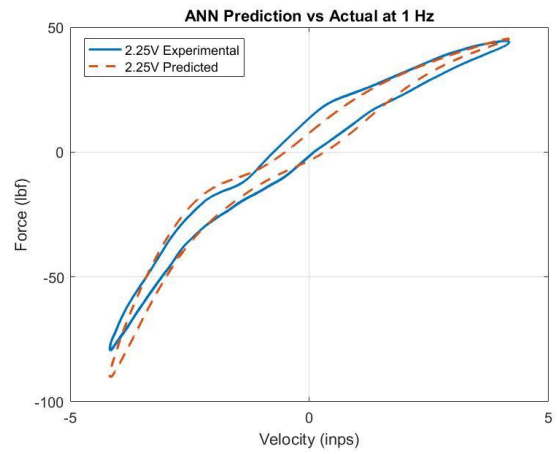
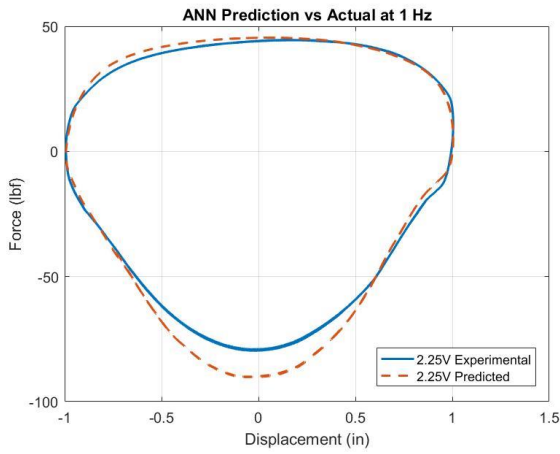


Figure 37: Predicted vs Actual Force at 1 Hz

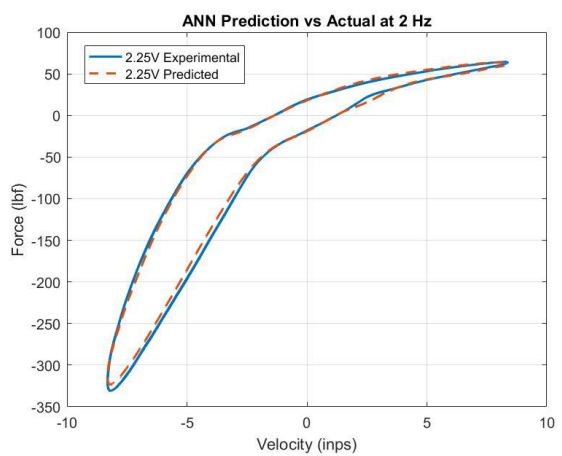
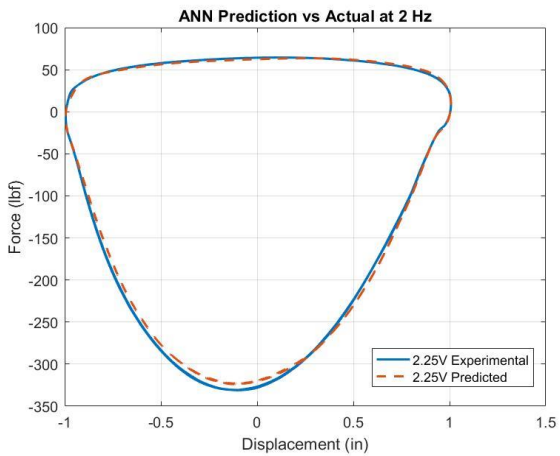


Figure 38: Predicted vs Actual Force at 2 Hz

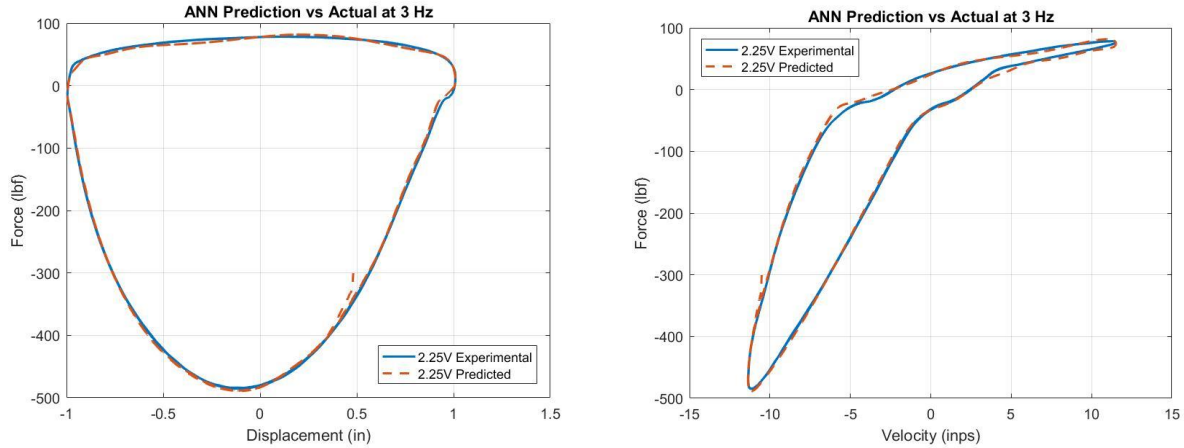


Figure 39: Predicted vs Actual Force at 3 Hz

Further, Table 4 shows the maximum error and the average % error in the predicted damper forces. It was observed that the ANN model did not deviate by more than 6% for most of the frequency range for which the model was developed. For very low frequencies, it can be argued that as the damper exhibits very low forces at low frequencies, even a maximum error of only about 9.8 lbf will not cause significant change in the vehicle dynamics despite it leading to a higher average % error.

Table 4: ANN Prediction error table

Test Frequency (Hz)	Maximum Error (lbf)	Average % Error
0.25	9.79	18.9
1	11.48	6.03
2	12.43	0.95
3	22.97	5.3

4.4 Summary and Discussion

The objective of the developed ANN is to predict the force the semi active damper would exert undergoing compression or rebound based on the instantaneous velocity, acceleration and voltage (damping coefficient). The damper force can be used in further simulations to study the modeled damper’s effect on vehicle ride and handling dynamics.

Following is a summary of the findings from the approach that was taken and the results that were achieved using the developed ANN damper model:

- The architecture was selected after reviewing previous studies and determining the significance of each input. Displacement was not chosen to be an input to avoid over constraining the network. Velocity and acceleration were chosen as inputs to provide accurate information of the dynamics. Voltage was chosen as an input to make it easier to implement multiple control strategies on the damper for further simulations. Back - propagation or ‘tapped delay’ techniques were not used to make the training and prediction faster as well as implementation of the network easier.
- The Levenberg – Marquardt algorithm was used to train the network as it led to the lowest MSE. Although the Scaled Conjugate algorithm took lesser time to train the network, the MSE was considerably higher and hence the network was not used.
- The ANN performed very well in the frequency range it was evaluated for with about 6% average error in its prediction. It can be argued that for very low speed tests (0.25 Hz - 0.5 Hz) the maximum prediction error was not significant enough to change the dynamics of a typical vehicle model considerably.

Based on the architecture discussed in Figure 34 the network can be expanded to a family of dampers by training it with more data from multiple dampers of the same vehicle segment and thus making the ANN model more flexible. After the evaluations, it was concluded the damper model predicted well for the frequencies up to 3 Hz which justifies its use to carry out evaluations for typical ride and handling dynamics for a vehicle.

5 SIMULATIONS AND RESULTS

After successful validation of the ANN damper model, the next steps were to carry out simulations to evaluate the feasibility of use of the model, implementation of a basic control strategy and effects of using a fully non-linear model for vehicle ride and handling simulations. A quarter car model was developed in Simulink with the conventional linear damper model replaced by the ANN damper model. A look up table damper model was also developed using the test data independently and was used to compare the performance of the ANN damper model. Further, a compact pickup RWD category vehicle was set up in CarSim with the default dampers replaced by the ANN damper model using the CarSim-Simulink Software-in-the-Loop approach. Standard ride and handling tests were simulated to evaluate the impact of using the non-linear ANN damper model.

5.1 Quarter Car Simulations

One of the most widely used model to study vehicle suspension dynamics is the quarter car model. Most suspension studies are initially carried out using the quarter car vehicle model and as per requirement the model is expanded to a half- car or full vehicle model [38]. For this study a quarter car model was developed in Simulink and the ANN damper model was integrated into it to evaluate its performance in computationally fast vehicle dynamics simulations.

5.1.1 Quarter Car Model Development

A quarter car model diagram for semi active suspension analysis has been illustrated in Figure 40. It consists of two masses, two springs and a semi active damper. The governing equations of motion for each mass were used to develop the quarter car model in Simulink. The parameters in the equations and their respective values used in the simulations have been explained in Table 5. The parameter values were chosen to be close to those for a typical compact pick-up truck as the ANN damper model was developed using a Chevrolet Silverado pick-up truck monotube damper.

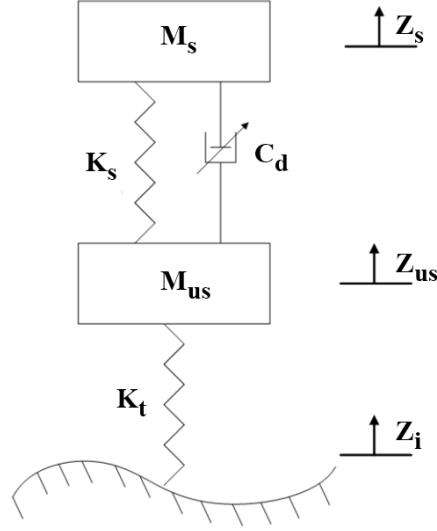


Figure 40: Point Contact Quarter Car Model

$$M_s \ddot{Z}_s + C_d(\dot{Z}_s - \dot{Z}_{us}) + K_s(Z_s - Z_{us}) = 0 \quad (13)$$

$$M_{us} \ddot{Z}_{us} - C_d(\dot{Z}_s - \dot{Z}_{us}) - K_s(Z_s - Z_{us}) + K_t(Z_{us} - Z_i) = 0 \quad (14)$$

Table 5: Quarter Car Parameter Definition

Terms	Parameter	Magnitude (units)
M_s	Sprung Mass	700 (Kg)
M_{us}	Unsprung Mass	40 (Kg)
K_s	Suspension Spring Stiffness	15 (kN/m)
K_t	Tire Stiffness	200 (kN/m)
C_d	Semi Active Suspension Damping	Variable (Ns/m)
Z_s	Sprung Mass Displacement	Changes during simulation (m)
Z_{us}	Unsprung Mass Displacement	Changes during simulation (m)
Z_i	Road Input	Changes during simulation (m)

The architecture of the Simulink model developed using equation (13) and (14) has been illustrated in Figure 41 and all quarter car results were obtained using this model.

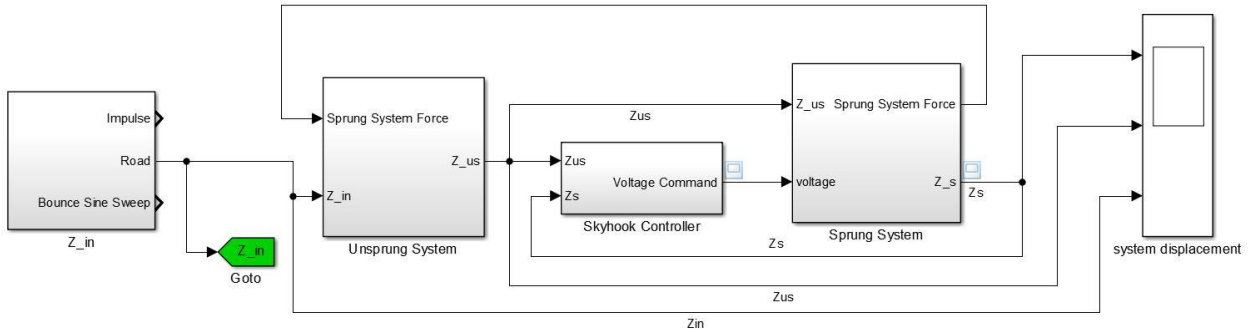


Figure 41: Simulink Quarter Car Model Architecture

It was important to use the ANN damper model in a way that was representative of an actual damper and avoid simulation errors, conceptual or computational. Therefore, the damper model was integrated into the quarter car model as shown in Figure 42.

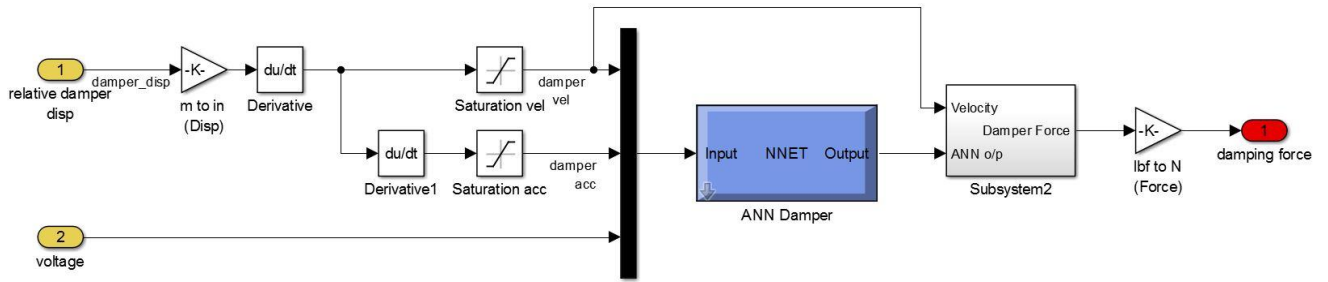


Figure 42: ANN Damper Model Integration

Nabagło, T. and J. Pietraszek [39] developed a neural network damper model and discussed about problems faced while using such models. Although, in this study, not all the same problems were exhibited by the developed ANN damper model, non-zero output for zero inputs was observed at some points in the simulation. Burnett, M., et al. [37] discussed this force in more detail and it was concluded that this was inherently due to the ‘breakaway’ load of the damper in the free condition. It was also argued that inserting extra data points which could ‘train’ the model to give a zero output for zero inputs was effective and significantly reduced the error to a point where the effects of the non-zero forces were negligible over the complete simulation. As already discussed in

Chapter 2 and Chapter 4, a neural network predicts with maximum accuracy when the inputs are within the range of the training data set or simply put reliable knowledge of the system only exists within the space defined by the training dataset. Saturation ports for velocity and acceleration were hence integrated to obtain a robust simulation model which does not ‘break down’ when provided with unexpected input data. The saturation levels of these ports can be increased by carrying out training using data for higher frequency range. The scope of this study is primarily limited to data obtained for up to 3 Hz. Conceptually, the model does not need to be changed to expand it for higher frequencies. Results of simulation show the above-mentioned techniques supported by literature led to successful integration of the ANN damper model into quarter car and CarSim simulation models.

Currently, for major part of suspension development in the industry, damper performance evaluation is carried out using a look up table based damper model which is developed using the frequency response data of the damper to be evaluated [37]. Therefore, lookup table damper models were developed for this study as well. To ensure the behavior of the semi active damper was comprehensively captured, lookup table damper models for both low damping and high damping were developed. Figure 43 shows the look up table models developed using the peak forces exhibited by the damper in the discussed modes for frequency ranging from 0-3 Hz. As expected from the trend seen in the data collected from the shock dynamometer, these developed models highlight the significant change in damper behavior for low and high damping modes; especially during rebound which is how the damper has been set up to behave in the first place. The trend seen in these lookup table damper curves agreed to the trend seen in previous literature [40]. Such models have been used in the industry for a long time as they are computationally inexpensive to use in simulations as well as provide a reliable and accurate estimate of the damper response. However, what these models fail to encompass are the full non-linearity and hysteresis which are an intrinsic part of the damper dynamics. This serves as the rationale to compare the ANN damper model to the look up table damper model and evaluate the similarities and significant differences that each of them led to in the simulation results.

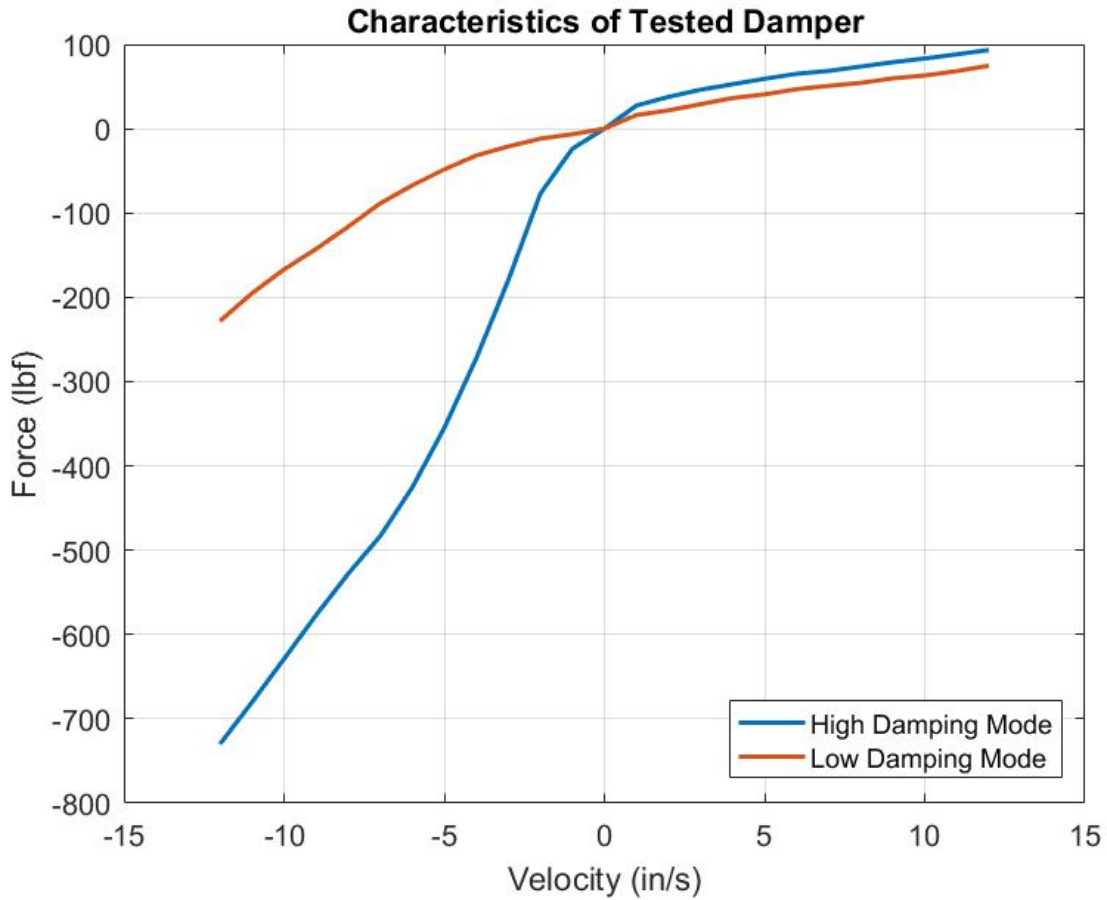
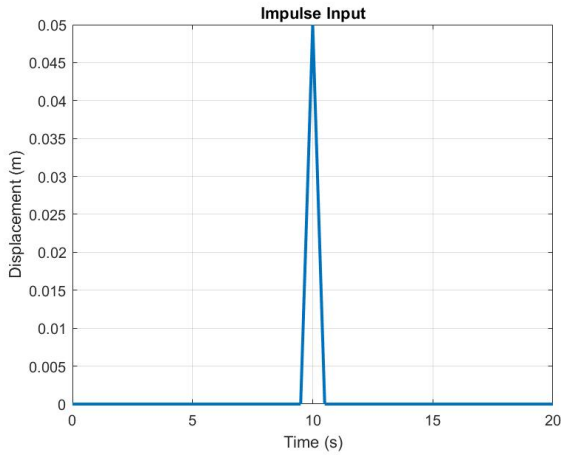


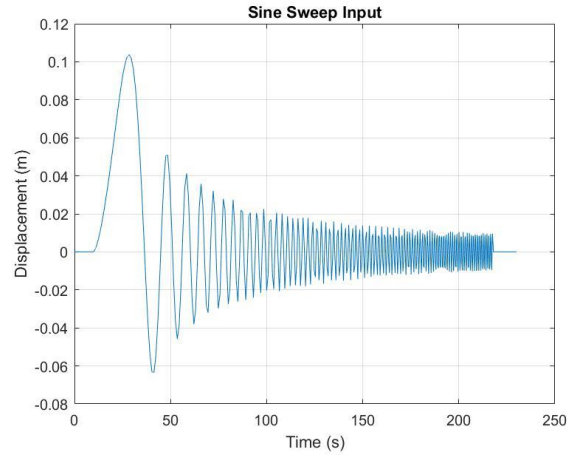
Figure 43: Lookup Table Damper Model

5.1.2 Tests and Results

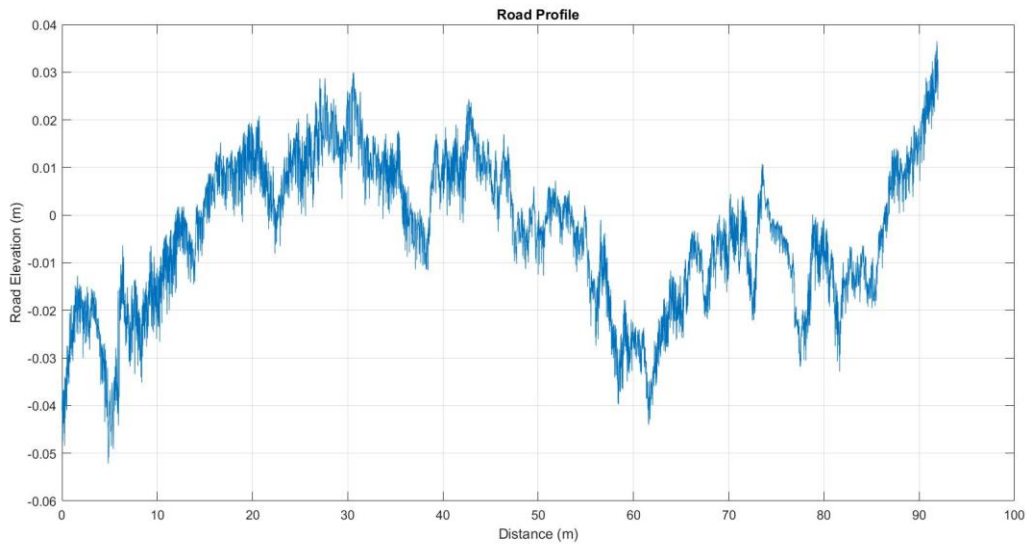
Once the simulation model was setup correctly and both the ANN damper model and look up table damper models were integrated successfully, the next step was to carry out multiple simulations for different standard road inputs to evaluate sprung mass response. The inputs used for the different simulations are illustrated in Figure 44.



(a)



(b)



(c)

Figure 44: Simulation Inputs (a) Impulse (b) Sine Sweep (c) Road Profile

The simulation using impulse input was primarily carried out as a robustness check as well as to evaluate effectiveness of the low and high damping modes of both the ANN damper model and the look up table damper model. The sprung mass response due to the impulse input is shown in Figure 45 and Figure 46. Both the damper models responded as expected after an impulse input for both low and high damping modes. Also, the lookup table damper model slightly overestimated the force generated by the damper as it lacks the hysteresis dynamics.

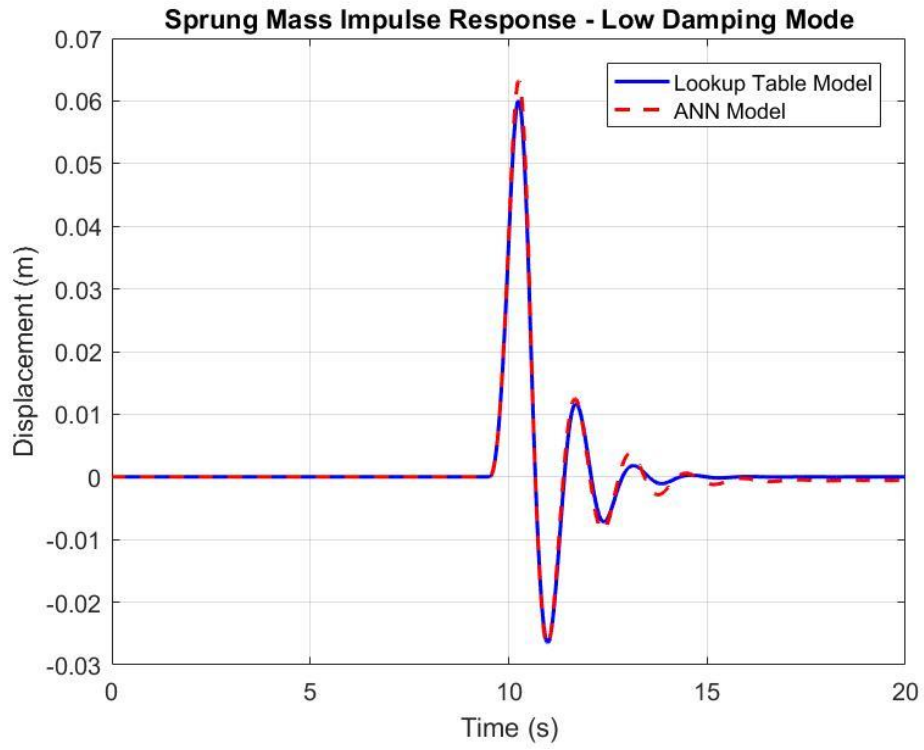


Figure 45: Sprung Mass Impulse Response – Low Damping Mode

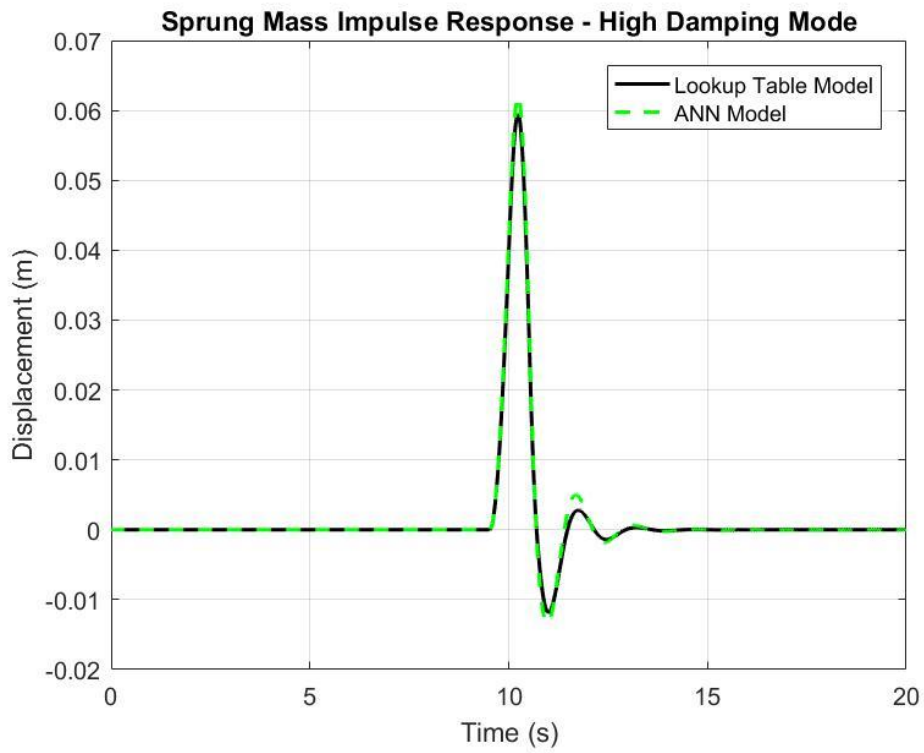


Figure 46: Sprung Mass Impulse Response – High Damping Mode

The most widely used input for ride analysis is the bounce sine sweep input. It provides a picture of the comfort over a range of frequencies, typically 0-20 Hz. Figure 47 and Figure 48 show the response of the quarter car model to the provided sine sweep input.

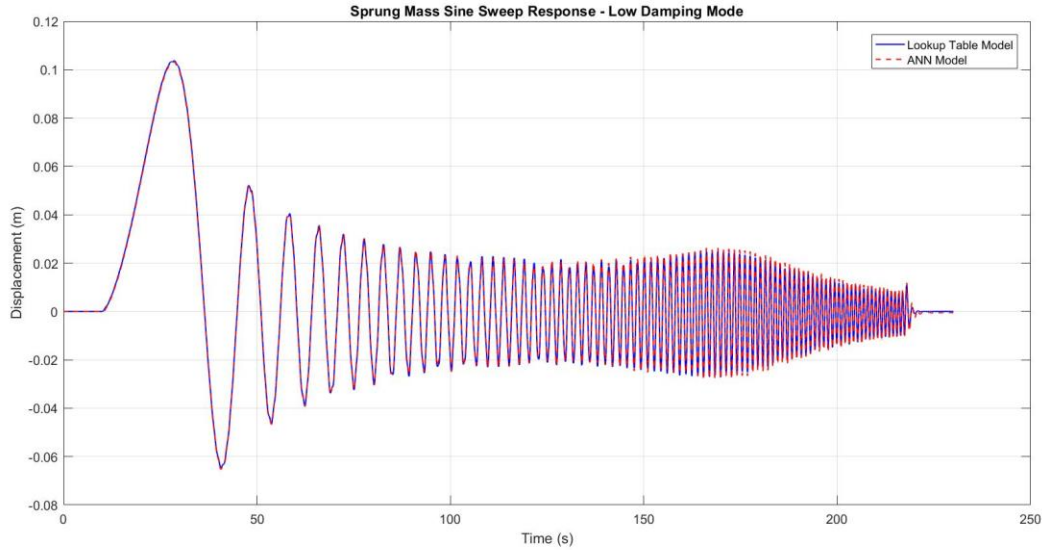


Figure 47: Sprung Mass Sine Sweep Response – Low Damping Mode

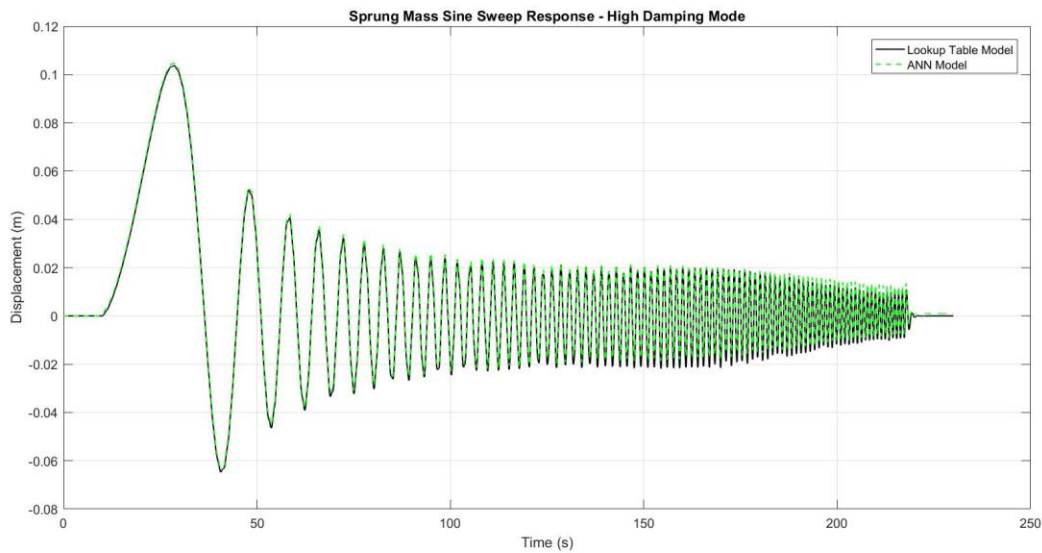


Figure 48: Sprung Mass Sine Sweep Response – High Damping Mode

Both damper models showed similar transmissibility characteristics and followed the sine sweep with consistency. In addition to ride analysis, the sine sweep test results also helped ensure model robustness and check for undesirable ANN damper model behavior such as noise introduction in the system during real time simulation. Table 6 shows the comparison of the RMS values of the

accelerations as well as displacement peak to RMS ratio experienced by the sprung mass using both damper models. It was observed that effects of non-linearity were more prominent in the high damping mode when damper dynamics had more effect on the sprung mass accelerations. As expected, RMS values for the ANN model were higher than for the lookup table model due the effect of hysteresis at higher frequency operation. Displacement peak to RMS ratio highlighted that the vertical dynamics of the sprung mass were not majorly affected using the two separate damper models.

Table 6: Sprung mass acceleration and displacement dynamics for sine sweep test

Damping Mode	Acceleration RMS (m/s²)		Displacement Peak to RMS	
	ANN	Lookup Table	ANN	Lookup Table
Low	0.1966	0.1837	3.5815	3.5980
High	0.2467	0.1644	3.6683	3.6444

An important part of evaluating damper performance is analysis of sprung mass dynamics using random road profiles. Therefore, as shown in Figure 44 (c), a rough road profile with a displacement RMS value of 0.016 m was used to carry out simulations and sprung mass displacement and acceleration dynamics were reported. The road profile was concatenated once to give an overall road profile about 184 m. Simulations were carried out for 10m/s and 20m/s to capture any major change in sprung mass dynamics with significant change in vehicle speed. Figure 49, Figure 50, Figure 51 and Figure 52 show the sprung mass response to the rough road input for low and high vehicle speeds. Ahmadian, M., et al. [41] discussed the well-known skyhook control strategy to reduce sprung mass displacements. Therefore, as the ANN damper model can support implementation of control strategies, this skyhook control strategy was implemented to demonstrate the developed model’s capability and effectiveness to be used for reduction in sprung mass displacement. Figure 53 and Figure 54 show the overall effect of the skyhook controller on the sprung mass displacement.

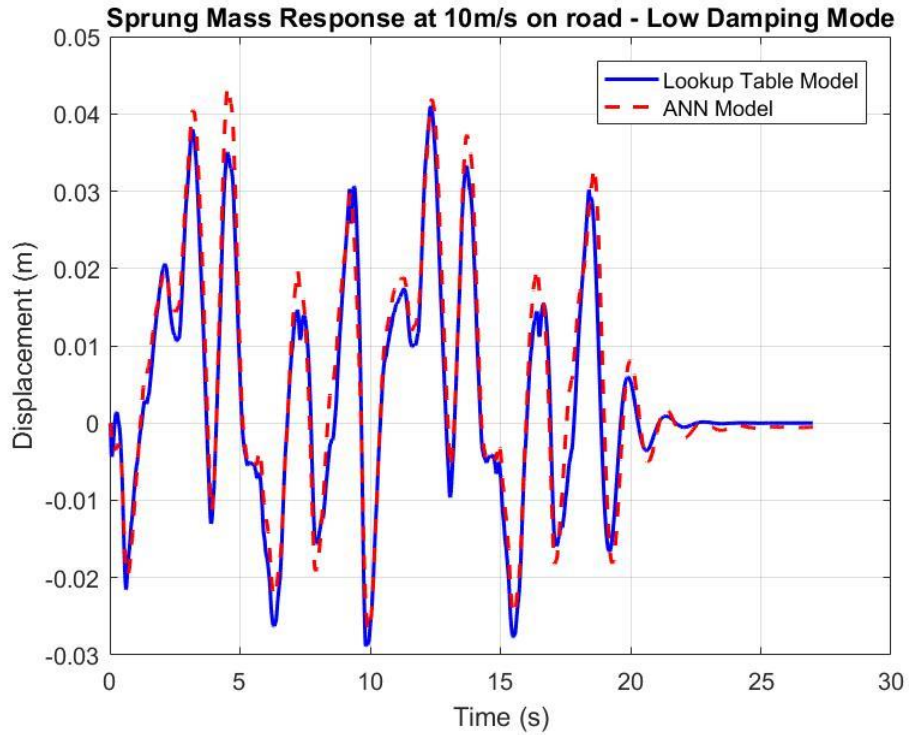


Figure 49: Sprung Mass Road Response at 10m/s – Low Damping Mode

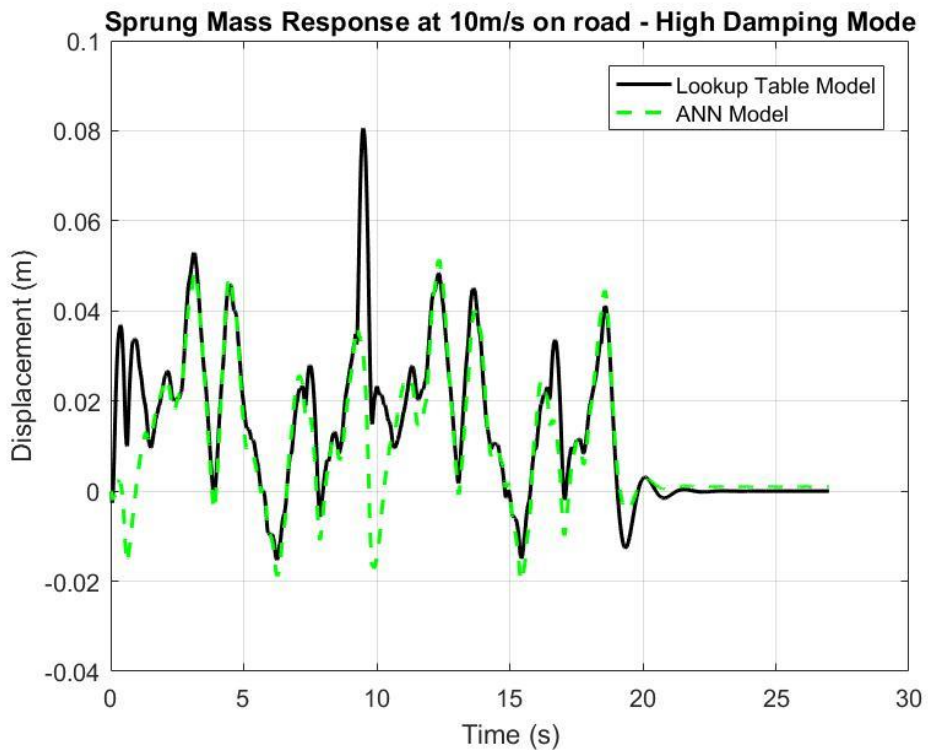


Figure 50: Sprung Mass Road Response at 10m/s – High Damping Mode

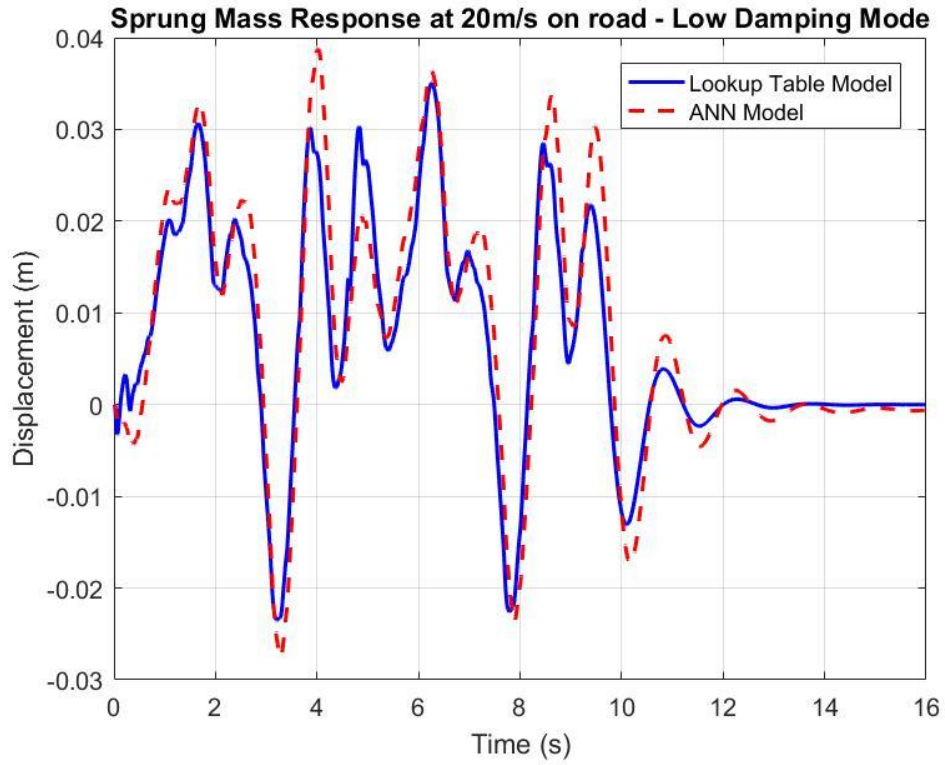


Figure 51: Sprung Mass Road Response at 20m/s – Low Damping Mode

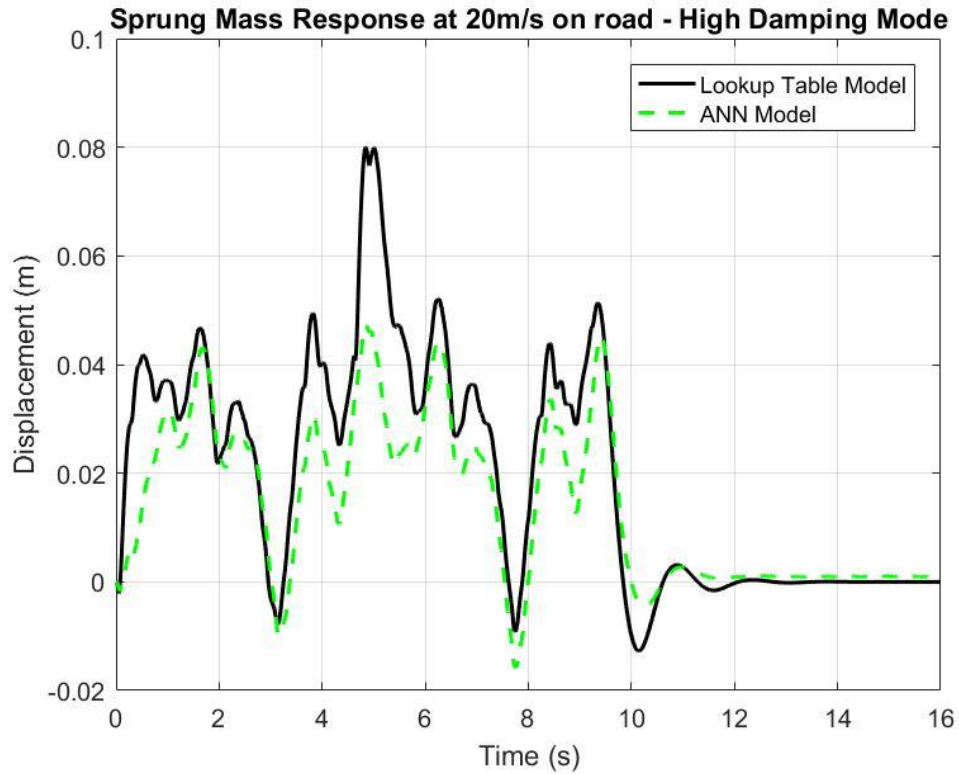


Figure 52: Sprung Mass Road Response at 20m/s – High Damping Mode

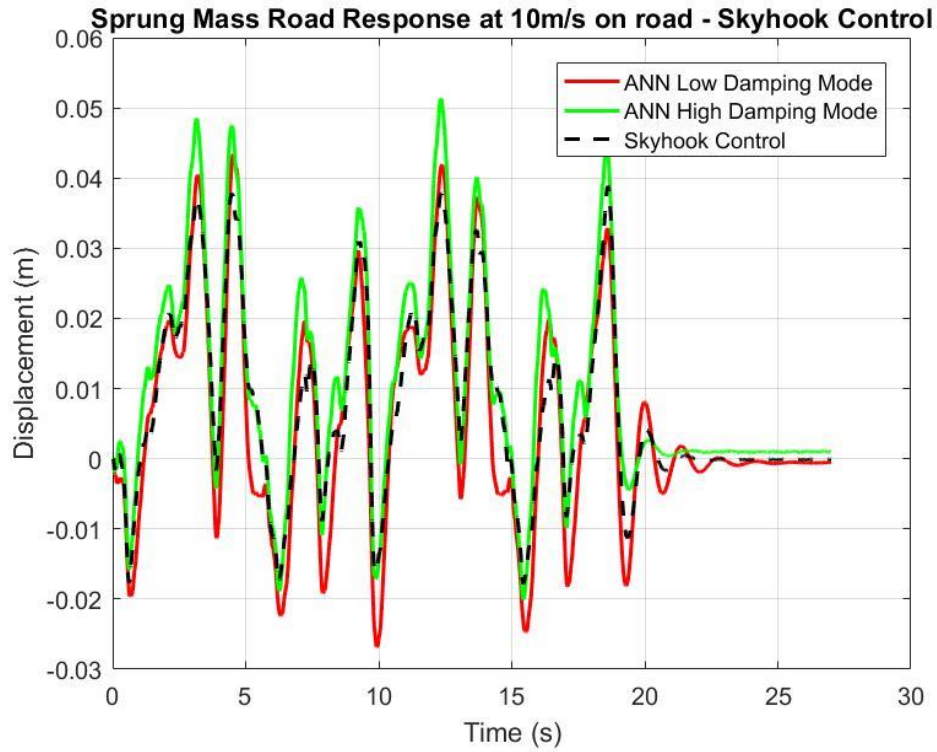


Figure 53: Sprung Mass Road Response at 10m/s – Skyhook Control

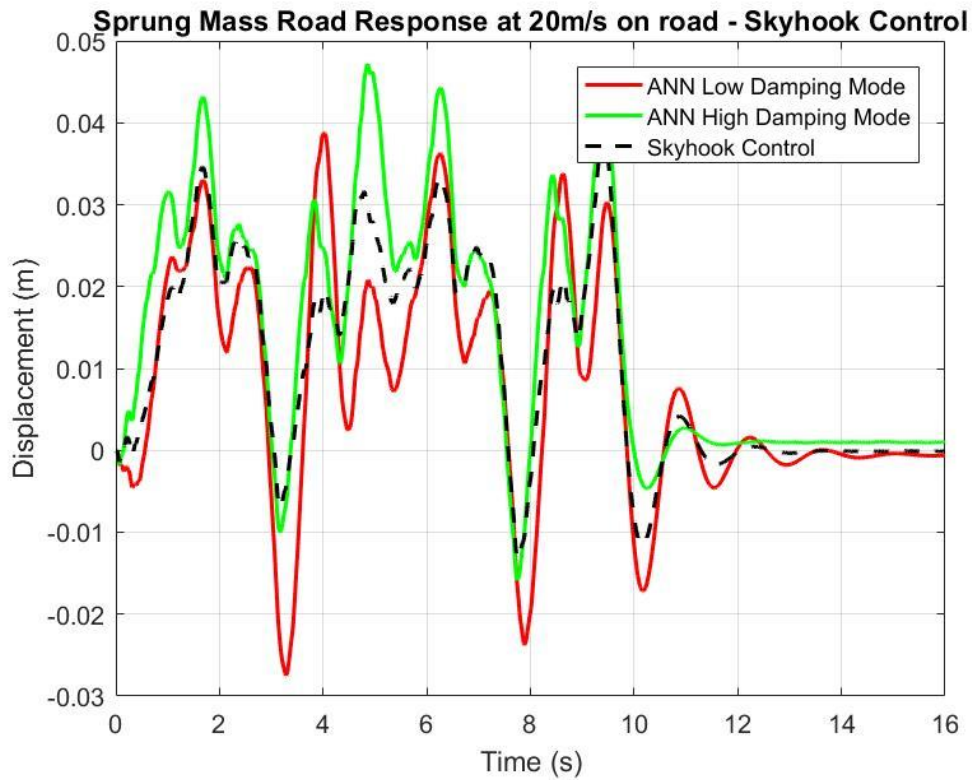


Figure 54: Sprung Mass Road Response at 20m/s – Skyhook Control

It was possible to observe the sprung mass dynamics changes when using the ANN damper model and the lookup table damper model. Figure 49 and Figure 51 highlight that during low damping mode, the effects on sprung mass displacement were essentially the same although it was observed that the lookup table damper model overestimated the stiffness of the damper for certain inputs. The effects of non-linearity were more visible when both damper models were used in the high damping mode as the stiffer dampers had much more impact on the sprung mass dynamics. Figure 50 and Figure 52 compare the response of the sprung mass and it could be observed that removing hysteresis effects from a damper model led to significant change in its estimation of damper forces especially during high frequency operation. Also, Figure 53 and Figure 54 established the effectiveness of the ANN damper model to be used with different control strategies to achieve minimum sprung mass displacement. Finally, a comparison of measure of energy transferred to the sprung mass using both damper models was carried out. As shown in Table 7, it was observed that the ANN Damper model led to lower acceleration RMS values for all conditions of vehicle speed and damper modes. This agrees with the conclusions reached by Gao, B., et al. [42].

Table 7: Acceleration RMS values for rough road input

Damping Mode	Low Vehicle Speed		High Vehicle Speed	
	ANN	Lookup Table	ANN	Lookup Table
Low	0.5633	0.6786	0.6546	0.8698
High	0.7482	1.0282	0.8676	1.2166

Hence, it can be established that ignoring the effects of damper hysteresis could lead to significant change in results of ride dynamics especially at higher frequencies where the damper behavior is dominated by non-linearity.

5.2 Full Vehicle Simulations

After successful validation and analysis of the developed ANN Damper model using quarter car simulations, the next step was to carry out full vehicle dynamics simulations to incorporate effects of damper performance on yaw, pitch and roll dynamics. CarSim, which is a widely-used commercial vehicle dynamics simulation program, was used to carry out full scale vehicle dynamics analysis. The ANN damper model was integrated using the Simulink- CarSim interface to set up a software-in-the-loop model, similar to ones developed in previous studies as well [43] and standard ride and handling tests were carried out to evaluate damper performance.

5.2.1 CarSim Model Development

As an extension to the analysis in the previous section, the objective was to evaluate the performance of the ANN damper model in a full vehicle model and compare it with test results using a lookup table damper model. Figure 55 illustrates the SIL setup which was used to carry out real time simulations by setting up a closed loop between CarSim and MATLAB/Simulink environment. The CarSim S-Function block was used in the Simulink environment to ensure real time data exchange of damper forces from the developed ANN damper model needed by CarSim and vehicle dynamics parameters from CarSim needed by the controller and damper model. The actual simulation setup has been shown in Figure 56.

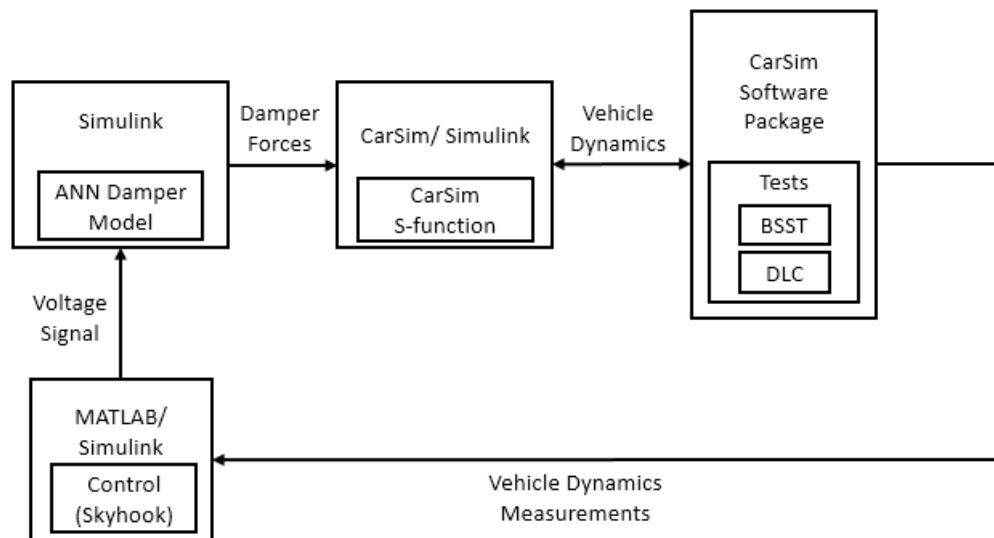


Figure 55: SIL Setup using CarSim with MATLAB/Simulink

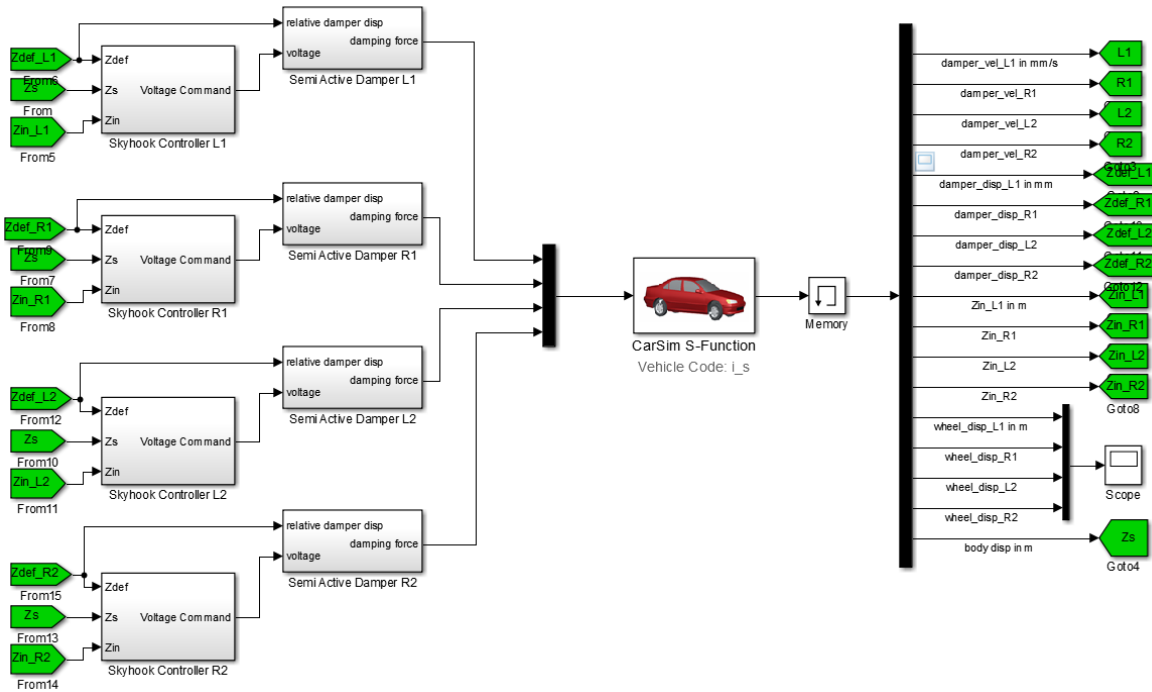
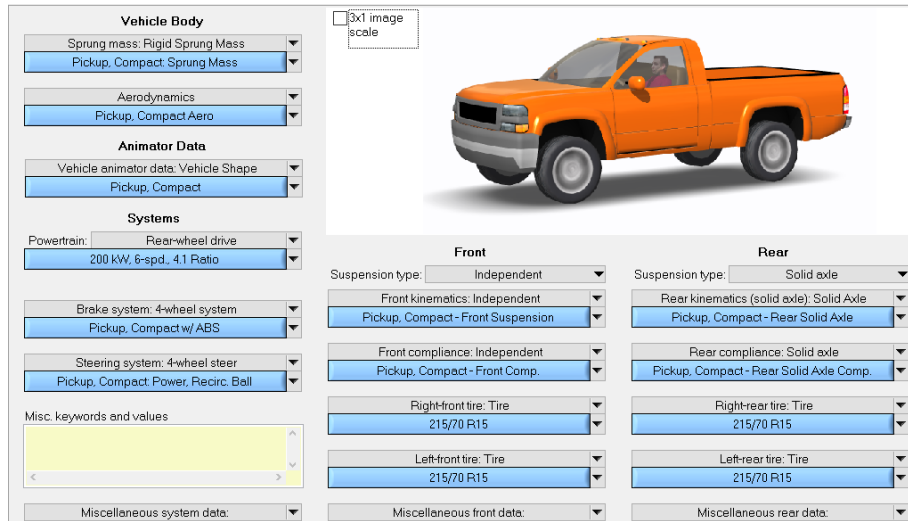
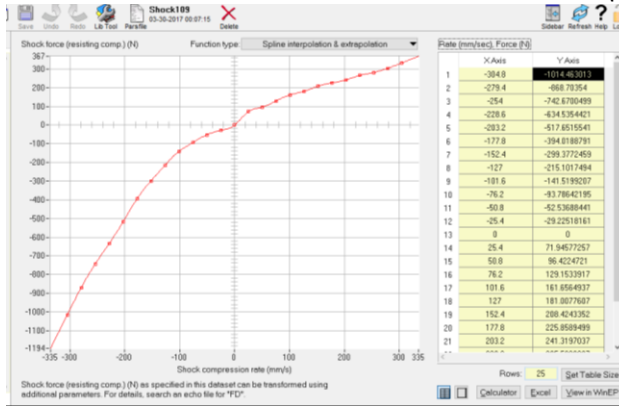


Figure 56: Actual CarSim-Simulink Setup

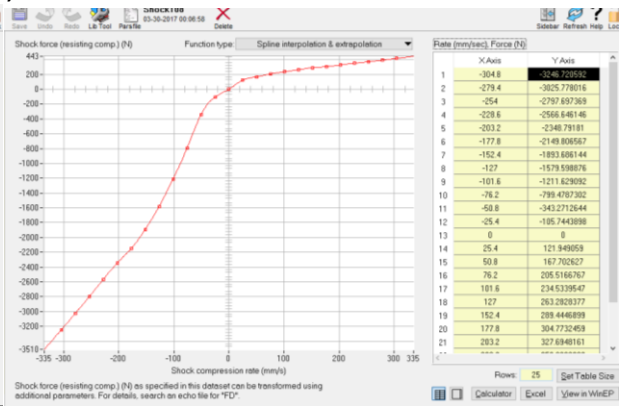
Unlike the quarter car model analysis, full vehicle model allowed for interaction between the four corners of the vehicle leading to generation of yaw, pitch and roll dynamics. The results of the vehicle simulation were obtained by carrying out specific tests for ride and handling dynamics evaluation. A ‘compact pickup-RWD’ class vehicle was selected for the full vehicle simulations. For comparison with the results obtained using the ANN damper model in the SIL test, CarSim default damper model for the selected vehicle class was replaced by the lookup table damper models (Figure 43). Figure 57 shows the CarSim vehicle model setup for the simulations and the integration of the lookup table damper models for both low and high damping modes. Previous studies suggested specific ride and handling tests for evaluating damper performances such as the Bounce Sine Sweep Test (BSST) and the Double Lane Change (DLC) test [44-46]. Therefore, the standard ride and handling tests were simulated and results obtained using both damper models were compared.



(a)



(b)



(c)

Figure 57: (a) CarSim Setup (b) Low Damping Lookup Table Damper
(c) High Damping Lookup Table Damper

5.2.2 Tests and Results

The bounce sine sweep test is generally used to carry out ride analysis and evaluate human comfort. Also, a double lane change test is generally used to evaluate handling of the vehicle. Both the tests have been explained briefly as below. These tests are pre-programmed in CarSim and were used to carry out separate simulations with both the ANN damper model and lookup table model in the loop respectively.

BSST: The vehicle is tested for comfort over a range of frequencies, generally 0-20 Hz. Suspension effectiveness is characterized by evaluating vehicle body vertical accelerations. Figure 58 (a) show a time varying snapshot of the test that was carried out for this study.

DLC–ISO 3888: The vehicle is tested for its handling dynamics over a series of lane change maneuvers as shown in Figure 58 (b) & (c). Suspension effectiveness is characterized by evaluating vehicle lateral acceleration, vehicle roll & roll rate and vehicle yaw rate. If no cones are overturned, the test is passed. The test was carried out at the CarSim standard vehicle speed of 120 km/h for this study.

CarSim has the capability to overlay multiple runs into one simulation and hence two vehicle simulations were overlaid onto each other with one vehicle fitted with the ANN damper model and the other fitted with the lookup table damper model. The voltage input of the ANN damper was fixed before each simulation with minimum and maximum voltage values to provide maximum and minimum damping respectively. The maximum and minimum damping look up table damper model simulations were overlaid accordingly and results were studied.

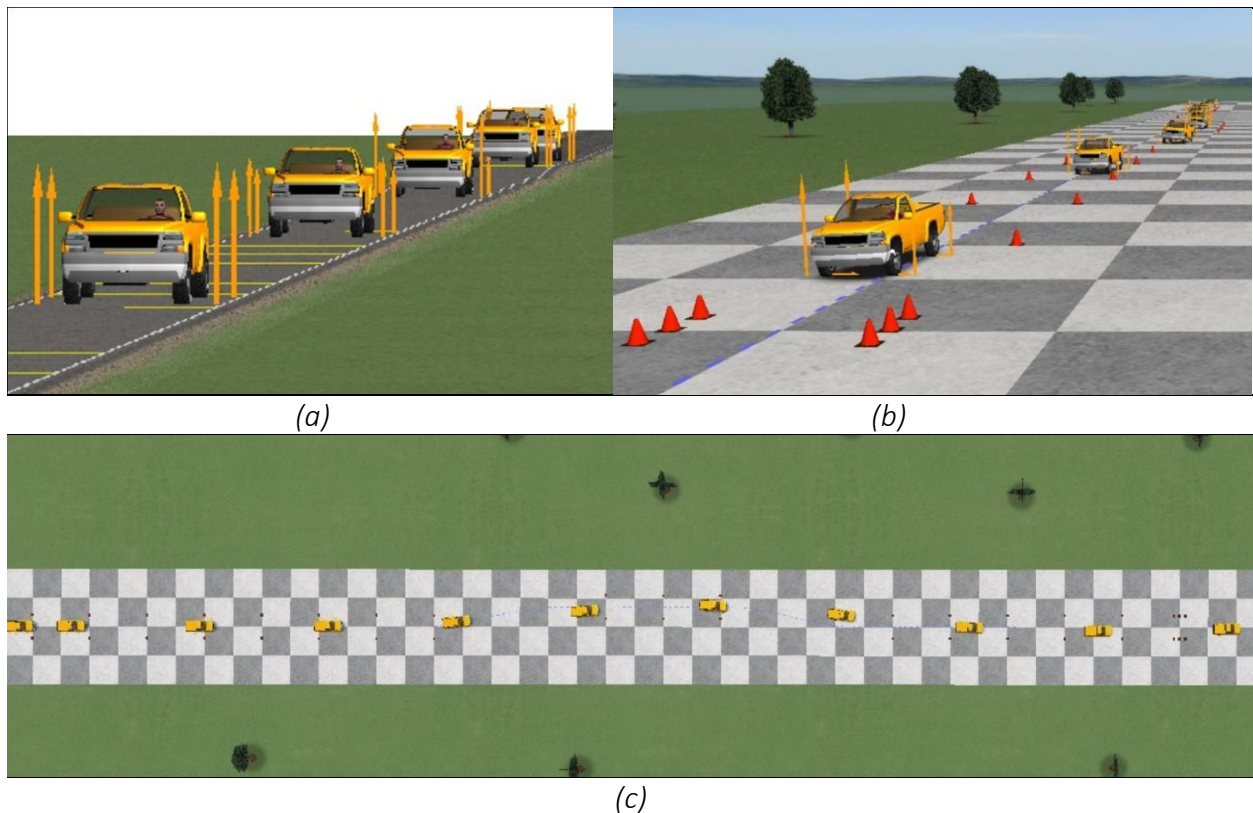


Figure 58: Tests carried out in CarSim: (a) BSST (b) DLC (c) DLC (Top View)

The vehicle body acceleration results from the BSST simulations have been shown in Figure 59. As expected and highlighted in the quarter car simulation results in Section 5.1.2, it was observed that the vehicle accelerations significantly varied between the two damper models being compared. The sprung mass acceleration RMS corresponding to the ANN damper model was found to be lesser which was clearly visible from the CarSim simulation results. The change in transmissibility was clearly distinguishable from about 8 second simulation point to the end of simulation. It was concluded that in a full vehicle model the effects of hysteresis in the damper model could not be neglected for ride analysis.

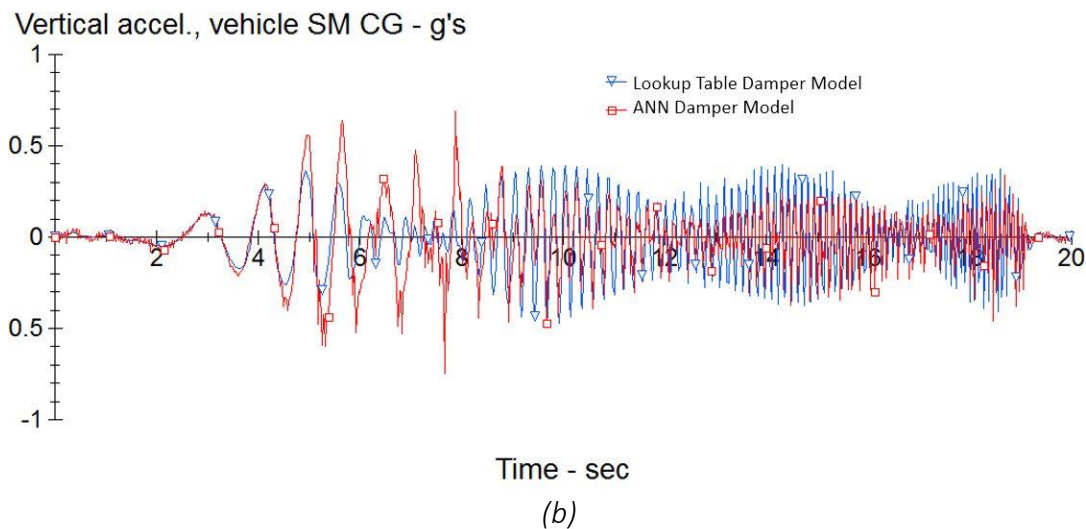
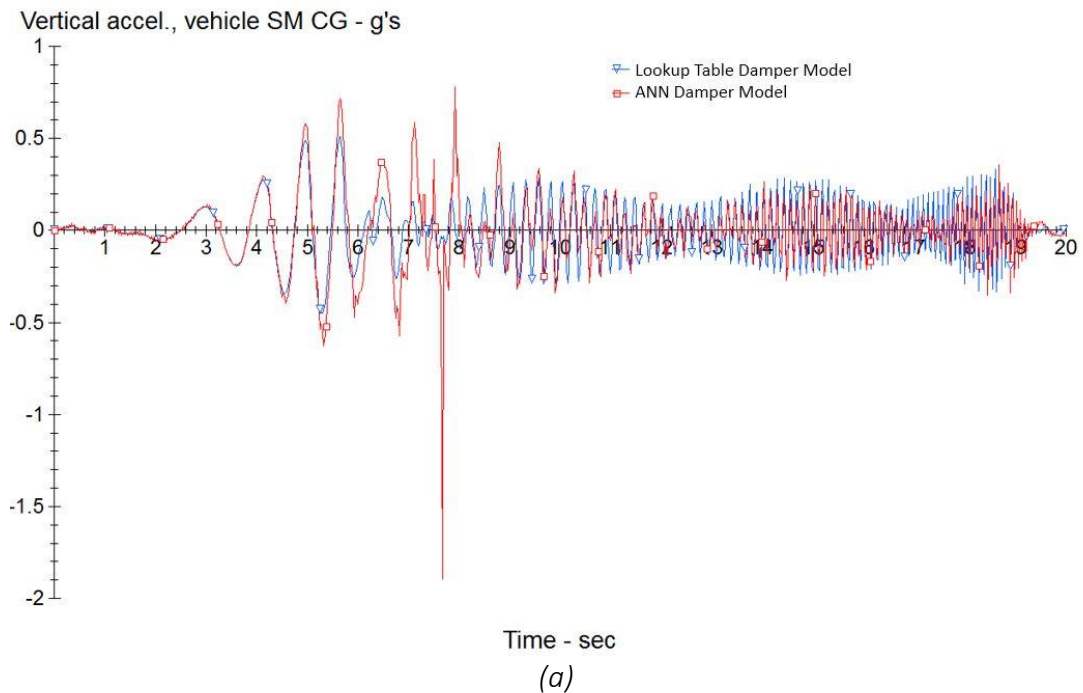


Figure 59: Vehicle Body Acceleration -BSST (a) Low Damping Mode (b) High Damping Mode

After ride analysis, the next step was to evaluate effect of the developed damper model on vehicle handling. A DLC maneuver generally gives a good idea on the vehicle's handling including yaw and roll dynamics as well as road holding capability. Tudon-Martinez, J. C., et al [46] studied the effects of multiple control strategies for an MR damper on the roll and road handling of the vehicle. Further, Jorge de-J, L.-S., et al [44] used the DLC to evaluate yaw rate, lateral acceleration, roll & roll rate and side slip angle of a semi active suspension equipped vehicle and compared the results to a baseline simulation. Therefore, DLC tests were performed using the pre-programmed setup of CarSim at a speed of 120Km/h. Figure 60 shows the simulation results and effects of using ANN damper model as compared to the lookup table model without hysteresis. The performance of the two damper models was nearly identical for all the tested parameters. The handling dynamics of the vehicle also did not significantly change while switching from a softer to a stiffer damper. A similar study by Calvo, J., et al. [47] in which effects of non-linear dampers on handling dynamics were studied, concluded that there was no major benefit of using a damper model with hysteresis to evaluate lateral and longitudinal vehicle dynamics. Liu, Y. and J. Zhang [48] and Simms, A. and D. Crolla [49] also concluded the ride dynamics results obtained using a damper model with hysteresis agreed more accurate to bench test results than using a piecewise linear damper but did not suggest whether this damper model with hysteresis would also be useful to carry out vehicle handling studies. Hence it was concluded that although using the ANN damper model with hysteresis did lead to some difference in vehicle handling simulations, they were not significant enough to justify the added complexity. Rather, damper models with hysteresis were found to be more beneficial for accurate ride and comfort analysis. An interesting complementary study would be to carry out handling tests with a damper model developed using higher frequency training data to see whether models trained using higher frequency test data would lead to significant change in vehicle handling.

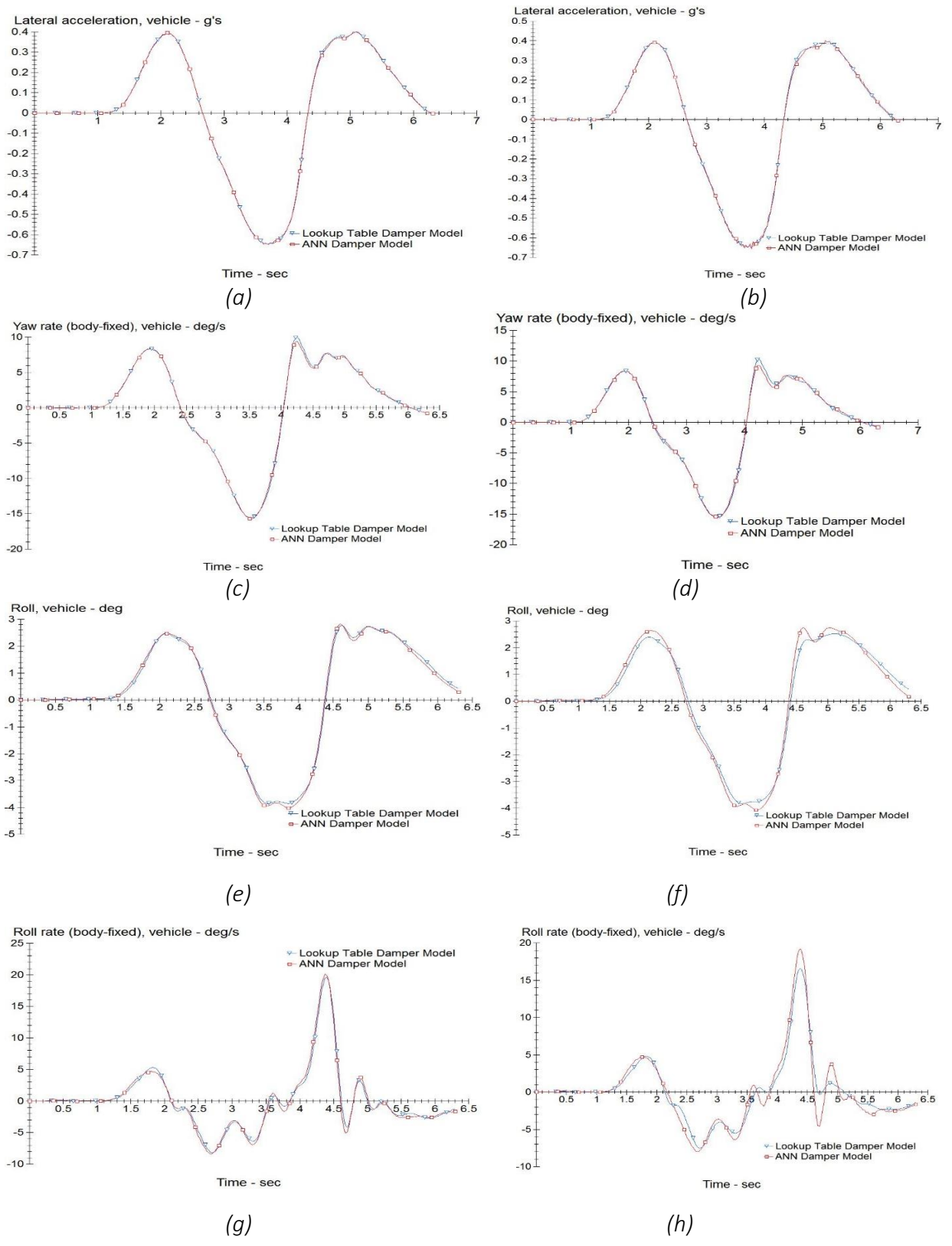


Figure 60: DLC Test Results – Low Damping:(a),(c),(e),(g) High Damping:(b),(d),(f),(h)

6 CONCLUSIONS AND FUTURE WORK

The aim of a vehicle suspension system is to provide good ride quality and human comfort while maintaining the desired road holding and handling capabilities of the vehicle. In general, there is always a compromise between achieving the desired ride & handling and hence an optimal balance between the two is targeted. Damper behavior plays a very important role to achieve the desired vehicle performance and more often damper tuning is based on trial and error methods. Dampers are inherently non-linear systems, especially when operating at higher frequencies. Multiple accurate physical damper models have been developed to simulate damper behavior but have not been very successful due to high computational costs and an overall added complexity to a vehicle dynamics simulation. Therefore, it is difficult to carry out damper tuning and achieve the desired ride and handling performance using these physical modeling techniques. The motivation behind this thesis was to explore a modeling technique to develop a damper model which would be computationally less demanding and would be able to encompass its non-linear behavior. Therefore, the first objective of this study was to develop and validate a damper model using artificial neural networks. The second objective of the study was to evaluate the feasibility and possible effects of using such a damper model in real time vehicle simulations.

Chapter 2 introduced the concept of neural networks and their working principle. In addition to classification of neural networks, the general training procedure and learning algorithms were discussed. Finally, the advantages and limitations of modeling a system using neural networks were discussed. It was concluded that neural networks can be trained using test data and obtain essentially ‘black box’ models of highly complex systems. It was also argued that this benefit also gave rise to a possible limitation since it is difficult to carry out system identification once a neural network ‘black box’ has been developed.

Chapter 4 discussed the architecture development of the ANN damper model, its efficient training and prediction capabilities. After examination of multiple neural network architectures, an MLP feedforward neural network with back propagation approach was selected to develop the desired damper model. After an iterative process the final architecture consisted of velocity, acceleration and voltage as inputs and damper force as the output. The network consisted of one hidden layer with 30 neurons with a sigmoidal activation function and was trained using data from tests carried

out from 0.25 to 3 Hz. Lowest RMSE was achieved using the Levenberg- Marquardt algorithm and was hence used for the training. It was demonstrated that the trained neural network predicted within 6% of the true values for an unseen set of data. Hence it was concluded that the developed ANN damper model was suitable to carry out evaluations for typical ride and handling dynamics for a vehicle.

Chapter 5 examined the feasibility of extending the ANN damper model to quarter car and full vehicle simulations for ride and handling analysis. A lookup table based damper model was developed using the test data for baseline comparison. After carrying out quarter car simulations for rough road input, it was demonstrated that the ANN damper model led to lower RMS values for the sprung mass accelerations in both low and high damping modes. Feasibility of using control strategies with the developed damper model was also established by demonstrating reduction in sprung mass displacement by using a skyhook control strategy. It was concluded it was not advisable to ignore non-linearity of the damper for high frequency ride analysis. Next, the damper model was integrated in an SIL test setup using CarSim and standard ride and handling tests were carried out. In agreement to the quarter car test results, the bounce sine sweep test (BSST) for ride analysis highlighted the significant difference in vehicle body accelerations using the ANN damper model vs the lookup table model. For evaluating vehicle handling and road holding capability, a double lane change (DLC) test was simulated. In agreement to previous literature it was found that non-linear damper dynamics for up to 3 Hz frequency operation did not majorly affect lateral acceleration, yaw and roll of the vehicle. The simulations led to the conclusion that using a non-linear damper model was beneficial for accurate ride and comfort analysis but not so much for handling analysis. It was also concluded that using a damper model developed using the neural network technique was easy to implement in real time simulations for full vehicle simulations.

To summarize, this study focused on developing a computationally inexpensive fully non-linear neural network based damper model and discussed the feasibility of using such a model in vehicle simulations. Both major objectives of the study were met as supported by results discussed in Chapter 4 and Chapter 5 respectively. It was believed that the present study helped in making another step towards possibility of accurate suspension tuning and testing through simulations.

There are several areas in which future work can be carried out. A brief overview of possible future work and recommendations is as below:

- Accurate modeling and testing of the solenoid valve can be carried out as any undesirable leakage or non-repeatability in valve operation could have an impact on the semi active damper system dynamics. Alternatively, an MR damper can be used to carry out a similar study without the need of bypass valves and problems associated with hydraulic leakage.
- A study on neural network architecture optimization can be carried out using constructive neural network and network pruning techniques. Such a study can avoid over constraining the network by providing too many inputs as well as further computational simplicity by decreasing the number of neurons in the hidden layer.
- A fair number of literature suggests using the ‘tapped delay’ based recurrent neural networks for modeling dynamic systems such as dampers. A study can be carried out exploring the feasibility of use of time delayed feedback based neural network models in a hardware-in-the-loop setup and a comparison be made with feedforward neural networks with no time delayed output feedback. It is believed that such a feedback system can result in error propagation in case of a bad output prediction.
- It is highly recommended that a study be carried out using the same philosophy as this study but training data be collected from a damper fitted in a shaker post setup simulated by random road inputs of varying roughness. The obtained model will be less prone to ‘breakdown’ due to exposure to high frequency input changes. Another advantage is elimination of need of a detailed damper test plan using a shock dynamometer.
- For this study, a single semi active damper was used to develop the ANN damper model. It is believed that it is possible to extend this study to obtain a damper model for a family of dampers by testing multiple dampers, including the changing variables as inputs to the neural network and finally realize a general fully non-linear damper model for a family of dampers. Temperature dependence can be an interesting input to study when moving into higher operating frequencies for suspension/wheel hop and tramp motion analysis.
- Evaluating the performance of advanced control strategies for semi active suspension systems was outside the scope of this particular study but it is possible to use a neural network based damper model to implement control strategies for ride as well as road holding on quarter car as well as full vehicle simulations.

BIBLIOGRAPHY

1. Xue, X., et al. *Study of art of automotive active suspensions*. in *Power Electronics Systems and Applications (PESA), 2011 4th International Conference on*. 2011. IEEE.
2. Simon, D. and M. Ahmadian, *Vehicle evaluation of the performance of magneto rheological dampers for heavy truck suspensions*. TRANSACTIONS-AMERICAN SOCIETY OF MECHANICAL ENGINEERS JOURNAL OF VIBRATION AND ACOUSTICS, 2001. **123**(3): p. 365-375.
3. Appleyard, M. and P. Wellstead, *Active suspensions: some background*. IEE Proceedings-Control Theory and Applications, 1995. **142**(2): p. 123-128.
4. Cao, J., et al., *State of the art in vehicle active suspension adaptive control systems based on intelligent methodologies*. IEEE transactions on intelligent transportation systems, 2008. **9**(3): p. 392-405.
5. Martins, I., et al. *Electromagnetic hybrid active-passive vehicle suspension system*. in *Vehicular Technology Conference, 1999 IEEE 49th*. 1999. IEEE.
6. Savaresi, S.M., et al., *Semi-active suspension control design for vehicles*. 2010: Elsevier.
7. Martins, I., et al. *Electromagnetic hybrid active-passive vehicle suspension system*. in *1999 IEEE 49th Vehicular Technology Conference (Cat. No.99CH36363)*. 1999.
8. Ekchian, J., et al., *A High-Bandwidth Active Suspension for Motion Sickness Mitigation in Autonomous Vehicles*. 2016, SAE Technical Paper.
9. Crosby, M., R. Harwood, and D. Karnopp, *Vibration control using semi-active force generators*. Journal of engineering for industry, 1974. **96**(2): p. 619-626.
10. Farjoud, A., *Physics-based modeling techniques for analysis and design of advanced suspension systems with experimental validation*. 2011.
11. Segel, L. and H. Lang, *The mechanics of automotive hydraulic dampers at high stroking frequencies*. Vehicle system dynamics, 1981. **10**(2-3): p. 82-85.
12. Reybrouck, K., *A non linear parametric model of an automotive shock absorber*. 1994, SAE Technical Paper.
13. Dominguez, A., R. Sedaghati, and I. Stiharu, *A new dynamic hysteresis model for magnetorheological dampers*. Smart materials and structures, 2006. **15**(5): p. 1179.
14. Kwok, N.M., et al., *Bouc–Wen model parameter identification for a MR fluid damper using computationally efficient GA*. ISA Transactions, 2007. **46**(2): p. 167-179.

15. Kwok, N.M., et al., *A novel hysteretic model for magnetorheological fluid dampers and parameter identification using particle swarm optimization*. *Sensors and Actuators A: Physical*, 2006. **132**(2): p. 441-451.
16. Zurada, J.M., *Introduction to artificial neural systems*. Vol. 8. 1992: West St. Paul.
17. McCulloch, W.S. and W. Pitts, *A logical calculus of the ideas immanent in nervous activity*. *The bulletin of mathematical biophysics*, 1943. **5**(4): p. 115-133.
18. Laudani, A., et al., *On training efficiency and computational costs of a feed forward neural network: a review*. *Computational intelligence and neuroscience*, 2015. **2015**: p. 83.
19. Ding, S., et al., *Evolutionary artificial neural networks: a review*. *Artificial Intelligence Review*, 2013. **39**(3): p. 251-260.
20. Wilamowski, B.M. *Neural network architectures and learning*. in *IEEE International Conference on Industrial Technology, 2003*. 2003.
21. Jaeger, H., *Tutorial on training recurrent neural networks, covering BPPT, RTRL, EKF and the "echo state network" approach*. Vol. 5. 2002: GMD-Forschungszentrum Informationstechnik.
22. Pearlmutter, B.A., *Gradient calculations for dynamic recurrent neural networks: a survey*. *IEEE Transactions on Neural Networks*, 1995. **6**(5): p. 1212-1228.
23. Ture, M., et al., *Comparing classification techniques for predicting essential hypertension*. *Expert Systems with Applications*, 2005. **29**(3): p. 583-588.
24. Kumar, K., et al., *Road Traffic Noise Prediction with Neural Networks-A Review*. *An international journal of optimization and control*. **2**(1): p. 29-37.
25. Riedmiller, M. and H. Braun. *A direct adaptive method for faster backpropagation learning: the RPROP algorithm*. in *IEEE International Conference on Neural Networks*. 1993.
26. Hagan, M.T. and M.B. Menhaj, *Training feedforward networks with the Marquardt algorithm*. *IEEE Transactions on Neural Networks*, 1994. **5**(6): p. 989-993.
27. Kermani, B.G., S.S. Schiffman, and H.T. Nagle, *Performance of the Levenberg–Marquardt neural network training method in electronic nose applications*. *Sensors and Actuators B: Chemical*, 2005. **110**(1): p. 13-22.
28. Kumar, P., S.N. Merchant, and U.B. Desai, *Improving performance in pulse radar detection using Bayesian regularization for neural network training*. *Digital Signal Processing*, 2004. **14**(5): p. 438-448.
29. MacKay, D.J., *Bayesian interpolation*. *Neural computation*, 1992. **4**(3): p. 415-447.
30. Sharma, S., S. Sudhir Kumar, and C. Pravin, *CONSTRUCTIVE NEURAL*

- NETWORKS: A REVIEW*. International journal of engineering science and technology, 2010. **2**(12): p. 7847-7855.
31. Janse van Rensburg, N., J.L. Steyn, and P.S. Els, *Time delay in a semi-active damper: modelling the bypass valve*. Journal of Terramechanics, 2002. **39**(1): p. 35-45.
 32. Gao, B., et al., *Non-linear modelling of a gas strut used in ground vehicle suspensions*. Transactions of the Institute of Measurement and Control, 2007. **29**(2): p. 159-183.
 33. Khalid, M., et al., *Nonlinear Identification of a Magneto-Rheological Damper Based on Dynamic Neural Networks*. Computer-aided civil and infrastructure engineering. **29**(3): p. 221-233.
 34. Priyandoko, G., M. Nizam, and I. Yahya. *Modeling of Magnetorheological Damper Using Back Propagation Neural Network*. in *Advanced Materials Research*. 2014. Trans Tech Publ.
 35. Chang, C.-C. and P. Roschke, *Neural Network Modeling of a Magnetorheological Damper*. Journal of Intelligent Material Systems and Structures, 1998. **9**(9): p. 755-764.
 36. Ekkachai, K., K. Tungpimolrut, and I. Nilkhamhang, *A novel approach to model magneto-rheological dampers using EHM with a feed-forward neural network*. Science Asia, 2012. **38**(4): p. 386-393.
 37. Burnett, M., A. Dixon, and J. Webb, *Damper Modelling Using Neural Networks*. AutoTechnology, 2003. **3**(4): p. 62-65.
 38. Lin, Y.J., J. Padovan, and Y.Q. Lu. *Toward better ride performance of vehicle suspension system via intelligent control*. in *[Proceedings] 1992 IEEE International Conference on Systems, Man, and Cybernetics*. 1992.
 39. Nabagło, T. and J. Pietraszek, *Neural network modeling of the semi-active magneto-rheological fluid damper*. Czasopismo Techniczne. Mechanika, 2010. **107**(2-M): p. 193-201.
 40. Cho, W., et al., *An investigation into unified chassis control scheme for optimised vehicle stability and manoeuvrability*. Vehicle System Dynamics, 2008. **46**(S1): p. 87-105.
 41. Ahmadian, M., X. Song, and S.C. Southward, *No-jerk skyhook control methods for semiactive suspensions*. Transactions of the ASME-L-Journal of Vibration and Acoustics, 2004. **126**(4): p. 580.
 42. Gao, B., et al. *Modelling of a novel gas strut using neural networks*. in *ASME 2004 International Mechanical Engineering Congress and Exposition*. 2004. American Society of Mechanical Engineers.
 43. Savaresi, S.M., E. Silani, and S. Bittanti, *Acceleration-driven-damper (ADD): An optimal control algorithm for comfort-oriented semiactive suspensions*. JOURNAL OF DYNAMIC SYSTEMS MEASUREMENT AND

- CONTROL-TRANSACTIONS OF THE ASME, 2005. **127**(2): p. 218-229.
44. Jorge de-J, L.-S., et al., *Influence of MR damper modeling on vehicle dynamics*. Smart Materials and Structures, 2013. **22**(12): p. 125031.
 45. Lozoya-Santos, J.d.-J., R. Morales-Menendez, and R.A. Ramirez-Mendoza, *Evaluation of on-off semi-active vehicle suspension systems by using the hardware-in-the-loop approach and the software-in-the-loop approach*. Proceedings of the Institution of Mechanical Engineers, Part D: Journal of Automobile Engineering, 2015. **229**(1): p. 52-69.
 46. Tudon-Martinez, J.C., J. Lozoya-Santos, and R. Morales-Menendez, *Efficiency of On-Off Semiactive Suspensions in a Pick-up Truck*. 2012.
 47. Calvo, J., et al., *Influence of a shock absorber model on vehicle dynamic simulation*. Proceedings of the Institution of Mechanical Engineers, Part D: Journal of Automobile Engineering, 2009. **223**(2): p. 189-203.
 48. Liu, Y. and J. Zhang, *Nonlinear dynamic responses of twin-tube hydraulic shock absorber*. Mechanics Research Communications, 2002. **29**(5): p. 359-365.
 49. Simms, A. and D. Crolla, *The influence of damper properties on vehicle dynamic behaviour*. 2002, SAE Technical Paper.